

# Gravitational redshift/blueshift of light emitted by geodesic test particles, frame-dragging and pericentre-shift effects, in the Kerr-Newman-de Sitter and Kerr-Newman black hole geometries

G. V. Kraniotis \*

University of Ioannina, Physics Department

Section of Theoretical Physics, GR- 451 10, Greece

February 4, 2020

## Abstract

We investigate the redshift and blueshift of light emitted by time-like geodesic particles in orbits around a Kerr-Newman-(anti) de Sitter (KN(a)dS) black hole. Specifically we compute the redshift and blueshift of photons that are emitted by geodesic massive particles and travel along null geodesics towards a distant observer-located at a finite distance from the KN(a)dS black hole. For this purpose we use the Killing-vector formalism and the associated first integrals-constants of motion. We consider in detail stable timelike equatorial circular orbits of stars and express their corresponding redshift/blueshift in terms of the metric physical black hole parameters (angular momentum per unit mass, mass, electric charge and the cosmological constant) and the orbital radii of both the emitter star and the distant observer. These radii are linked through the constants of motion along the null geodesics followed by the photons since their emission until their detection and as a result we get closed form analytic expressions for the orbital radius of the observer in terms of the emitter radius, and the black hole parameters. In addition, we compute exact analytic expressions for the frame dragging of timelike spherical orbits in the KN(a)dS spacetime in terms of multivariable generalised hypergeometric functions of Lauricella and Appell. We apply our exact solutions of timelike non-spherical polar KN geodesics for the computation of frame-dragging, pericentre-shift, orbital period for the orbits of S2 and S14 stars

---

\*email: gkraniot@cc.uoi.gr

within the  $1''$  of SgrA\*. Last but not least we derive a very elegant and novel exact formula for the periapsis advance for a test particle in a non-spherical polar orbit in KNdS black hole spacetime in terms of Jacobi's elliptic function  $\text{sn}$  and Lauricella's hypergeometric function  $F_D$ .

## 1 Introduction

General relativity (GR) has triumphed all experimental tests so far which cover a wide range of field strengths and physical scales that include: those in large scale cosmology [17],[18], the prediction of solar system effects like the perihelion precession of Mercury with a very high precision [1],[19], the recent discovery of gravitational waves in Nature [35],[36], as well as the observation of the shadow of the M87 black hole [24], see also [5].

The orbits of short period stars in the central arcsecond (S-stars) of the Milky Way Galaxy provide the best current evidence for the existence of supermassive black holes [2],[3].

In a series of papers we solved exactly timelike and null geodesics in Kerr and Kerr-(anti) de Sitter black hole spacetimes [6], [7],[20], and null geodesics and the gravitational lens equations in electrically charged rotating black holes in [8]. We also computed in [6] elegant closed form analytic solutions for the general relativistic effects of periapsis advance, Lense-Thirring precession, orbital and Lense-Thirring periods and applied our solutions for calculating these GR-effects for the observed orbits of S-stars. The shadow of the Kerr and charged Kerr black holes were computed in [9],[7] and [8] respectively.

One of the targets of observational astronomers of the galactic centre is to measure the gravitational redshift predicted by the theory of general relativity [10]. In the Schwarzschild spacetime geometry the ratio of the frequencies measured by two stationary clocks at the radial positions  $r_1$  and  $r_2$  is given by [15]:

$$\frac{\nu_1}{\nu_2} = \frac{\sqrt{1 - 2GM/r_2}}{\sqrt{1 - 2GM/r_1}}, \quad (1)$$

where  $G$  is the gravitational constant and  $M$  is the mass of the black hole. Recently, the redshift/blueshift of photons emitted by test particles in timelike circular equatorial orbits in Kerr spacetime were investigated in [31].

It is the purpose of this paper to extend our previous results on relativistic observables and compute for the *first time* the redshift and blueshift of light emitted by timelike geodesic particles in orbits around the Kerr-Newman-(anti) de Sitter (KN(a)dS) black hole. In addition, we derive new exact analytic expressions for the pericentre-shift and frame-dragging for non-spherical non-equatorial (polar) timelike KNdS and KN black hole orbits. Moreover, we derive novel exact expressions for the frame dragging effect for particles in spherical, non-equatorial orbits in KNdS and KN black hole geometries. These results will be of interest to the observational astronomers of the Galactic centre [2],[3] whose aim is to measure experimentally, the relativistic effects predicted by the theory of General Relativity [30] for the observed orbits of short-period stars-the

so called S-stars in our Galactic centre. During 2018, the close proximity of the star S2 (S02) to the supermassive Galactic centre black hole allowed the first measurements of the relativistic redshift observable by the GRAVITY collaboration [11] and the UCLA Galactic centre group whose astrometric measurements were obtained at the W.M. Keck Observatory [12]<sup>1</sup>.

One of the most fundamental exact non-vacuum solutions of the gravitational field equations of general relativity is the Kerr-Newman black hole [14]. The Kerr-Newman (KN) exact solution describes the curved spacetime geometry surrounding a charged, rotating black hole and it solves the coupled system of differential equations for the gravitational and electromagnetic fields [14] (see also [15]).

The KN exact solution generalised the Kerr solution [16], which describes the curved spacetime geometry around a rotating black hole, to include a net electric charge carried by the black hole.

A more realistic description should include the cosmological constant [17], [18], [19] [8], [7] [21], [22], [23], [27], [28].

Taking into account the contribution from the cosmological constant  $\Lambda$ , the generalisation of the Kerr-Newman solution is described by the Kerr-Newman de Sitter (KNdS) metric element which in Boyer-Lindquist (BL) coordinates is given by [37], [38], [40], [39] (in units where  $G = 1$  and  $c = 1$ ):

$$ds^2 = \frac{\Delta_r^{KN}}{\Xi^2 \rho^2} (dt - a \sin^2 \theta d\phi)^2 - \frac{\rho^2}{\Delta_r^{KN}} dr^2 - \frac{\rho^2}{\Delta_\theta} d\theta^2 - \frac{\Delta_\theta \sin^2 \theta}{\Xi^2 \rho^2} (adt - (r^2 + a^2)d\phi)^2 \quad (2)$$

$$\Delta_\theta := 1 + \frac{a^2 \Lambda}{3} \cos^2 \theta, \quad \Xi := 1 + \frac{a^2 \Lambda}{3}, \quad (3)$$

$$\Delta_r^{KN} := \left(1 - \frac{\Lambda}{3} r^2\right) (r^2 + a^2) - 2Mr + e^2, \quad (4)$$

$$\rho^2 = r^2 + a^2 \cos^2 \theta, \quad (5)$$

where  $a, M, e$ , denote the Kerr parameter, mass and electric charge of the black hole, respectively. The KN(a)dS metric is the most general exact stationary black hole solution of the Einstein-Maxwell system of differential equations. This is accompanied by a non-zero electromagnetic field  $F = dA$ , where the vector potential is [41], [40]:

$$A = -\frac{er}{\Xi(r^2 + a^2 \cos^2 \theta)} (dt - a \sin^2 \theta d\phi). \quad (6)$$

---

<sup>1</sup>Observational work is ongoing towards the detection of the periastron shift of the star S2 and the discovery of putative closer stars-in the central milliarcsecond of SgrA\* supermassive black hole [13], which could allow an astrometric measurement of the black hole spin as envisaged e.g. in [6].

The KN(a)dS dynamical system of geodesics is a completely integrable system<sup>2</sup> as was shown in [38],[37],[41],[20] and the geodesic differential equations take the form:

$$\int \frac{dr}{\sqrt{R'}} = \int \frac{d\theta}{\sqrt{\Theta'}}, \quad (7)$$

$$\rho^2 \frac{d\phi}{d\lambda} = -\frac{\Xi^2}{\Delta_\theta \sin^2 \theta} (aE \sin^2 \theta - L) + \frac{a\Xi^2}{\Delta_r^{KN}} [(r^2 + a^2)E - aL], \quad (8)$$

$$c\rho^2 \frac{dt}{d\lambda} = \frac{\Xi^2(r^2 + a^2)[(r^2 + a^2)E - aL]}{\Delta_r^{KN}} - \frac{a\Xi^2(aE \sin^2 \theta - L)}{\Delta_\theta}, \quad (9)$$

$$\rho^2 \frac{dr}{d\lambda} = \pm \sqrt{R'}, \quad (10)$$

$$\rho^2 \frac{d\theta}{d\lambda} = \pm \sqrt{\Theta'}, \quad (11)$$

where

$$R' := \Xi^2 [(r^2 + a^2)E - aL]^2 - \Delta_r^{KN} (\mu^2 r^2 + Q + \Xi^2 (L - aE)^2), \quad (12)$$

$$\Theta' := [Q + (L - aE)^2 \Xi^2 - \mu^2 a^2 \cos^2 \theta] \Delta_\theta - \Xi^2 \frac{(aE \sin^2 \theta - L)^2}{\sin^2 \theta}. \quad (13)$$

Null geodesics are derived by setting  $\mu = 0$ . The proper time  $\tau$  and the affine parameter  $\lambda$  are connected by the relation  $\tau = \mu\lambda$ . In the following we use geometrised units,  $G = c = 1$ , unless it is stipulated otherwise. The first integrals of motion  $E$  and  $L$  are related to the isometries of the KNdS metric while  $Q$  (Carter's constant) is the hidden integral of motion that results from the separation of variables of the Hamilton-Jacobi equation.

The material of the paper is organised as follows: In Sec. 2 we consider the Killing vector formalism and the corresponding conserved quantities in Kerr-Newman-(anti) de Sitter spacetime. In Sec.3 we consider equatorial circular geodesics in KN(a)dS spacetime and derive novel expressions for the specific energy and specific angular momentum for test particles moving in such orbits, see equations (26) and (27). Typical behaviour of these functions is displayed in Fig.1-Fig.17. Furthermore, we investigate the stability of such timelike circular equatorial geodesics in Kerr-Newman-de Sitter spacetime and derive a new condition that restricts their radii, namely the inequality (33). In Sec. 4 we provide general expressions for the redshift/blueshift that emitted photons by massive particles experience while travelling along null geodesics towards an observer located far away from their source by making use of the Killing vector formalism. In Sec.4.1 we derive novel exact analytic expressions for the redshift/blueshift of photons for circular and equatorial emitter/detector orbits around the Kerr-Newman-(anti) de Sitter black hole-see equations (65) and (66) respectively. In the procedure we take into account the bending of light due to the field of the Kerr-Newman-(anti)de Sitter black hole at the moment of detection by the

---

<sup>2</sup>This is proven by solving the relativistic Hamilton-Jacobi equation by the method of separation of variables.

observer. We derive the corresponding frequency shifts for circular equatorial orbits in Kerr-de Sitter spacetime in Sec. 4.1.1. We also examine the particular case when the detector is located far away from the source. In Sec.5 we study non-equatorial orbits in rotating charged black hole spacetimes. Specifically, we compute in closed analytic form the frame-dragging for test particles in time-like spherical orbits in the Kerr-Newman and Kerr-Newman-de Sitter black hole spacetimes-equations (81),theorem 4 and (89) respectively. The former equation (KN case) involves the ordinary Gauß hypergeometric function and Appell's  $F_1$  two-variable hypergeometric function, while the latter (KNdS case) is expressed in terms of Lauricella's  $F_D$  and Appell's  $F_1$  generalised multivariate hypergeometric functions [33]. In Sec. 5.4 and 5.4.1 we derive new exact solutions for the Lense-Thirring precession and the orbital period for a test particle in a polar non-spherical orbit around a Kerr-Newman black hole, Eqns(95) and (100) respectively. In Sec.5.5 & 5.6 we derive new closed form analytic expressions for the periapsis advance for test particles in non-spherical polar orbits in KN and KNdS spacetimes respectively. In the latter case we derive a novel, very elegant, exact formula in terms of Jacobi's elliptic function  $\text{sn}$  and Lauricella's hypergeometric function  $F_D$  of three variables-see equation (117). The exact results of sections 5.4,5.4.1,5.5, are applied for the computation of the relativistic effects for frame-dragging, pericentre shift and the orbital periods for the observed orbits of stars S2 and S14 in the central arcsecond of Milky way, assuming that the galactic centre supermassive black hole is a Kerr-Newman black hole.

## 2 Particle orbits and Killing vectors formalism in Kerr-Newman-(anti)de Sitter spacetime

From the condition for the invariance of the metric tensor:

$$0 = \xi^\alpha \frac{\partial g_{\mu\nu}}{\partial x^\alpha} + \frac{\partial \xi^\alpha}{\partial x^\mu} g_{\alpha\nu} + \frac{\partial \xi^\beta}{\partial x^\nu} g_{\mu\beta}, \quad (14)$$

under the infinitesimal transformation:

$$x'^\alpha = x^\alpha + \epsilon \xi^\alpha(x), \quad \text{with } \epsilon \rightarrow 0 \quad (15)$$

it follows that whenever the metric is independent of some coordinate a constant vector in the direction of that coordinate is a Killing vector . Thus the generic metric:

$$ds^2 = g_{tt}dt^2 + 2g_{t\phi}dtd\phi + g_{\phi\phi}d\phi^2 + g_{rr}dr^2 + g_{\theta\theta}d\theta^2, \quad (16)$$

possesses two commuting Killing vector fields:

$$\xi^\mu = (1, 0, 0, 0) \text{ timelike Killing vector,} \quad (17)$$

$$\psi^\mu = (0, 0, 0, 1) \text{ rotational Killing vector.} \quad (18)$$

According to Noether's theorem to every continuous symmetry of a physical system corresponds a conservation law. In a general curved spacetime, we

can formulate the conservation laws for the motion of a particle on the basis of Killing vectors. We can prove that if  $\xi_\nu$  is a Killing vector, then for a particle moving along a geodesic, the scalar product of this Killing vector and the momentum  $P^\nu = \mu \frac{dx^\nu}{d\tau}$  of the particle is a constant [15]:

$$\xi_\nu P^\nu = \text{constant} \quad (19)$$

Due to the existence of these Killing vector fields (17),(18) there are two conserved quantities the total energy and the angular momentum per unit mass at rest of the test particle <sup>3</sup>:

$$E = \frac{\tilde{E}}{\mu} = g_{\mu\nu} \xi^\mu U^\nu = g_{tt} U^t + g_{t\phi} U^\phi, \quad (20)$$

$$L = \frac{\tilde{L}}{\mu} = -g_{\mu\nu} \psi^\mu U^\nu = -g_{\phi t} U^t - g_{\phi\phi} U^\phi. \quad (21)$$

Thus, the photon's emitter is a probe massive test particle which geodesically moves around a rotating electrically charged cosmological black hole in the spacetime with a four-velocity:

$$U_e^\mu = (U^t, U^r, U^\theta, U^\phi)_e. \quad (22)$$

The conservation law (19) also applies to photon moving in the curved spacetime. Thus, if the spacetime geometry is time independent, the photon energy  $P_0$  is constant. In section 4.1 we will extract the redshift/blueshift of photons from this conservation law.

### 3 Equatorial circular orbits in Kerr-Newman spacetime with a cosmological constant

It is convenient to introduce a dimensionless cosmological parameter:

$$\Lambda' = \frac{1}{3} \Lambda M^2, \quad (23)$$

and set  $M = 1$ . For equatorial orbits Carter's constant  $Q$  vanishes. For the following discussion, it is useful to introduce new constants of motion, the specific energy and specific angular momentum:

$$\hat{E} \equiv \frac{\Xi E}{\mu}, \quad (24)$$

$$\hat{L} \equiv \frac{\Xi L}{\mu}. \quad (25)$$

---

<sup>3</sup>As we mentioned already in the introduction, the charged Kerr solution possesses another hidden constant, Carter's constant  $Q$ . Alternatively, the complete integrability of the geodesic equations in KN(a)dS spacetime can be understood as follows: The Kerr-Newman family of spacetimes possesses in addition to the two Killing vectors a Killing tensor field  $K_{\alpha\beta}$ . This tensor can be expressed in terms of null tetrads (e.g. see eqn (7) in [45]) which implies the existence of a constant of motion  $K = K_{\mu\nu} U^\mu U^\nu$ . This is related to Carter's constant by:  $K \equiv Q + (L - aE)^2$ . See also [42],[43].

This is equivalent to setting  $\mu = 1$ . Thus for reasons of notational simplicity we omit the caret for the specific energy and specific angular momentum in what follows.

Equatorial circular orbits correspond to local extrema of the effective potential. Equivalently, these orbits are given by the conditions  $R'(r) = 0, dR'/dr = 0$ , which have to be solved simultaneously. Following this procedure, we obtain the following novel equations for the specific energy and the specific angular momentum of test particles moving along equatorial circular orbits in KN(a)dS spacetime:

$$E_{\pm}(r; \Lambda', a, e) = \frac{e^2 + r(r-2) - r^2(r^2 + a^2)\Lambda' \pm a\sqrt{r^4\left(\frac{1}{r^3} - \Lambda'\right) - e^2}}{r\sqrt{2e^2 + r(r-3) - a^2r^2\Lambda' \pm 2a\sqrt{r^4\left(\frac{1}{r^3} - \Lambda'\right) - e^2}}}, \quad (26)$$

$$L_{\pm}(r; \Lambda', a, e) = \frac{\pm(r^2 + a^2)\sqrt{r^4\left(\frac{1}{r^3} - \Lambda'\right) - e^2} - 2ar - ar^2\Lambda'(r^2 + a^2) + ae^2}{r\sqrt{2e^2 + r(r-3) - a^2r^2\Lambda' \pm 2a\sqrt{r^4\left(\frac{1}{r^3} - \Lambda'\right) - e^2}}} \quad (27)$$

The reality conditions connected with equations (26) and (27) are given by the inequalities:

$$2e^2 + r(r-3) - a^2r^2\Lambda' \pm 2a\sqrt{r^4\left(\frac{1}{r^3} - \Lambda'\right) - e^2} \geq 0 \quad (28)$$

$$\Leftrightarrow \frac{2e^2}{r^2} + \frac{r-3}{r} - a^2\Lambda' \pm 2a\sqrt{\frac{1}{r^3} - \Lambda' - \frac{e^2}{r^4}} \geq 0, \quad (29)$$

and

$$1 - \Lambda'r^3 \geq e^2/r. \quad (30)$$

For zero electric charge  $e = 0$  equations (26),(27) reduce correctly to those in Kerr-anti de Sitter (KadS) spacetimes [25]. For zero electric charge and zero cosmological constant ( $\Lambda = e = 0$ ) equations (26),(27) reduce correctly to the corresponding ones in Kerr spacetime [26].

In the figures 1-17, for concrete values of the electric charge and the cosmological parameter we present the radial dependence of the specific energy and specific angular momentum for various values of the black hole's spin. For the cosmological parameter  $\Lambda'$  we choose the values  $\Lambda' = 10^{-5}, 10^{-4}, 10^{-3}$  as well as their negative counterparts. For stellar mass black holes, and positive cosmological constant this corresponds to  $\Lambda \sim 10^{-15}\text{cm}^{-2} - 10^{-13}\text{cm}^{-2}$ . For supermassive black holes such as at the centre of Galaxy M87 with mass  $M_{\text{BH}}^{M87} = 6.7 \times 10^9$  solar masses [24] the value of  $\Lambda' = 10^{-5}$  corresponds to the value for the cosmological constant:  $\Lambda = 3.06 \times 10^{-35}\text{cm}^{-2}$ .

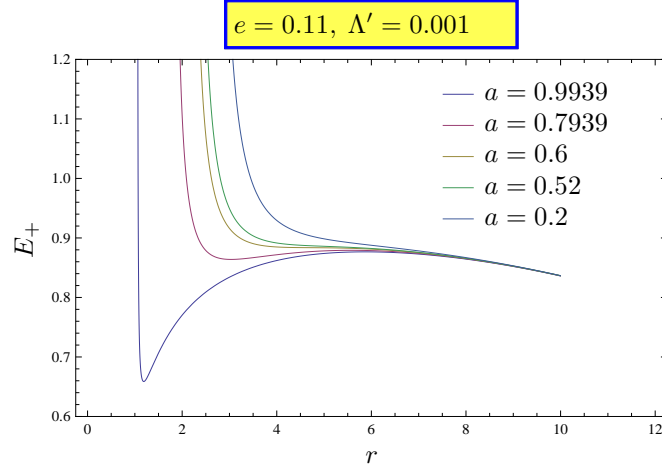


Figure 1: Specific energy  $E_+$  for  $e = 0.11, \Lambda' = 0.001$  for different values for the Kerr parameter.

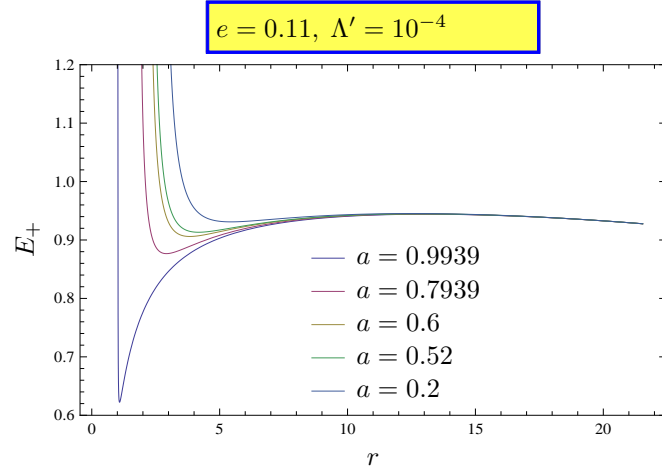


Figure 2: Specific energy  $E_+$  for  $e = 0.11, \Lambda' = 0.0001$  for different values for the Kerr parameter.



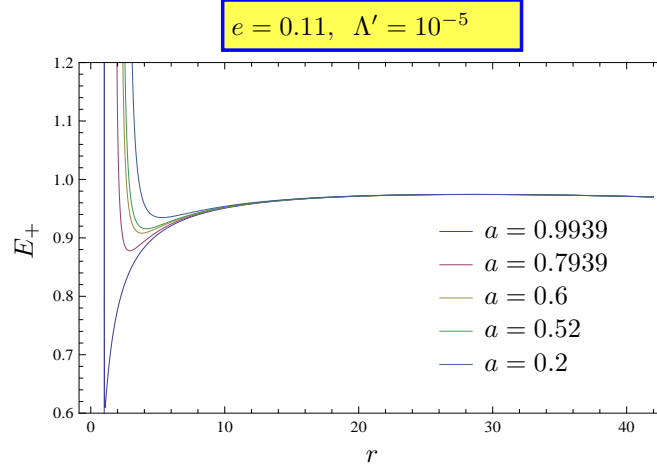


Figure 3: Specific energy  $E_+$  for  $e = 0.11, \Lambda' = 0.00001$  for different values for the Kerr parameter.

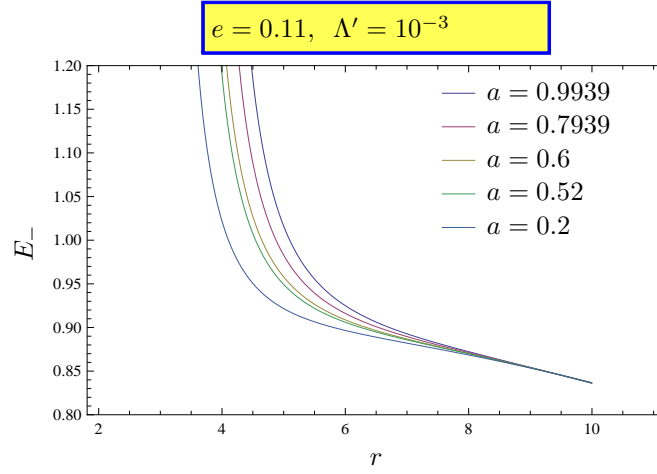


Figure 4: Specific energy  $E_-$  for  $e = 0.11, \Lambda' = 0.001$  for different values for the Kerr parameter.

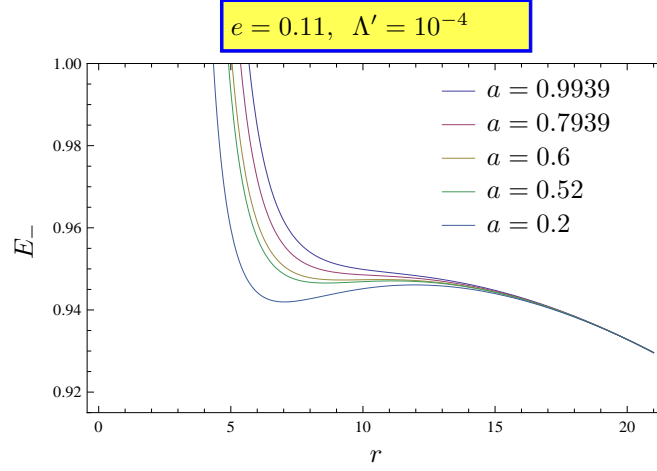


Figure 5: Specific energy  $E_-$  for  $e = 0.11, \Lambda' = 0.0001$  for different values for the Kerr parameter.

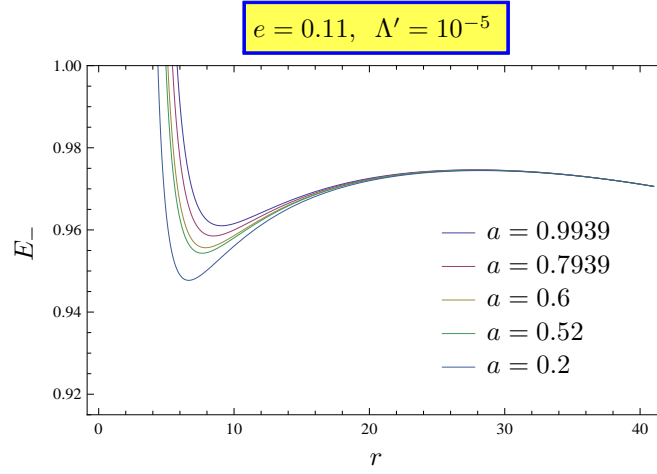


Figure 6: Specific energy  $E_-$  for  $e = 0.11, \Lambda' = 0.00001$  for different values for the Kerr parameter.

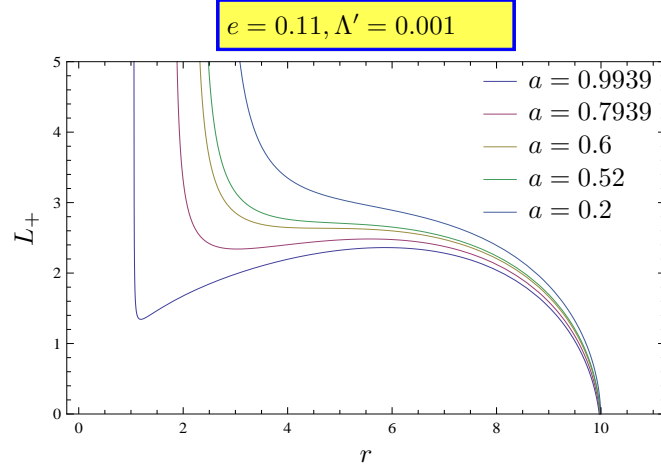


Figure 7: Specific angular momentum  $L_+$  for  $e = 0.11, \Lambda' = 0.001$  for different values for the Kerr parameter.

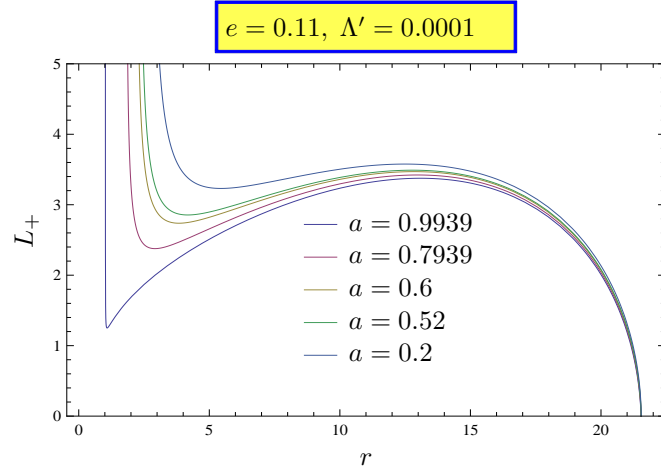


Figure 8: Specific angular momentum  $L_+$  for  $e = 0.11, \Lambda' = 0.0001$  for different values for the Kerr parameter.

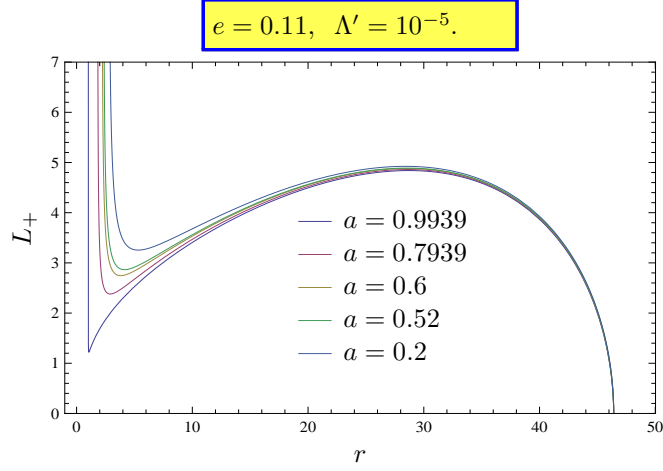


Figure 9: Specific angular momentum  $L_+$  for  $e = 0.11, \Lambda' = 10^{-5}$  for different values for the Kerr parameter.

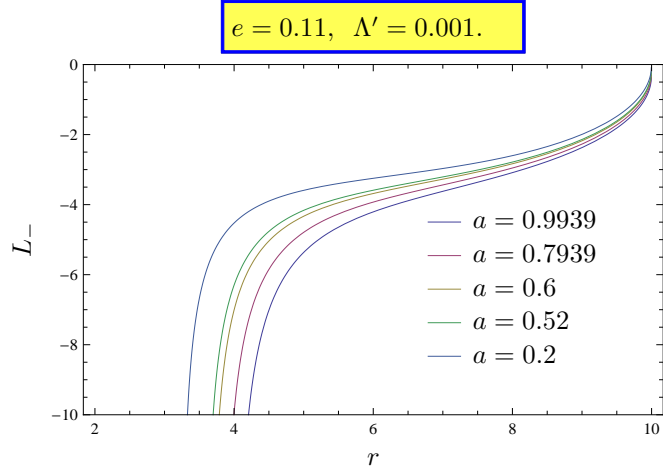


Figure 10: Specific angular momentum  $L_-$  for  $e = 0.11, \Lambda' = 10^{-3}$  for different values for the Kerr parameter.

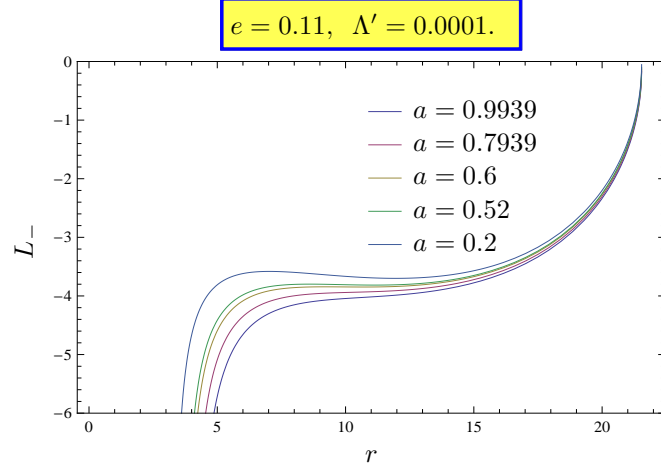


Figure 11: Specific angular momentum  $L_-$  for  $e = 0.11, \Lambda' = 10^{-4}$  for different values for the Kerr parameter.

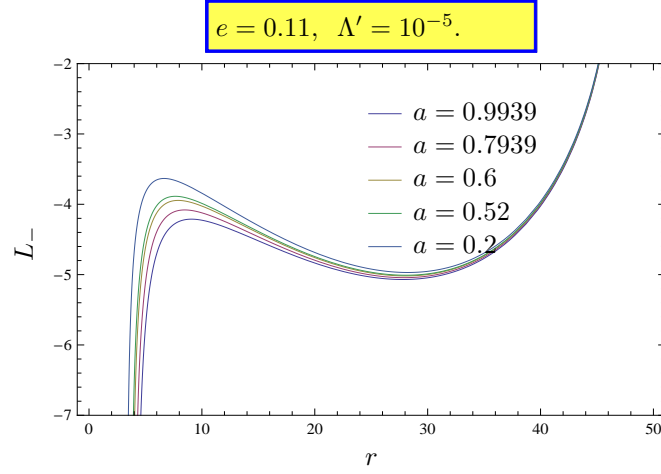


Figure 12: Specific angular momentum  $L_-$  for  $e = 0.11, \Lambda' = 10^{-5}$  for different values for the Kerr parameter.

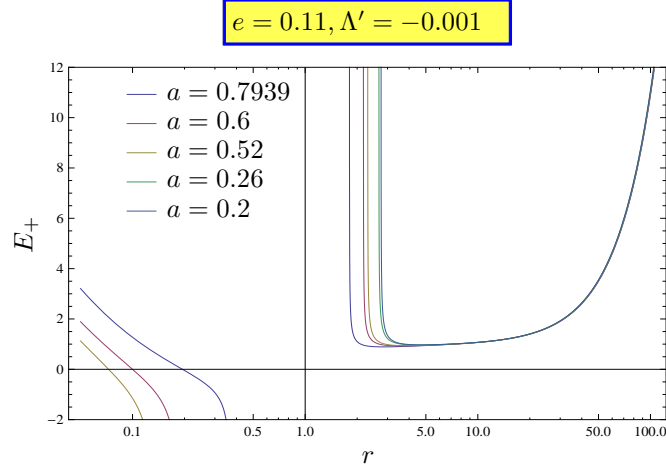


Figure 13: Specific energy  $E_+$  for  $e = 0.11, \Lambda' = -0.001$  for different values for the Kerr parameter.

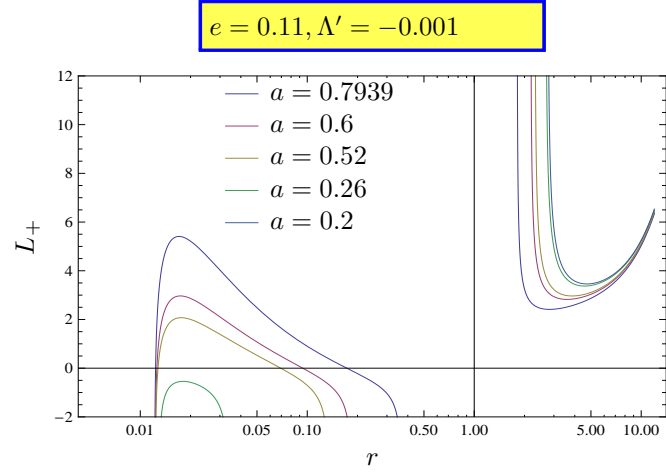


Figure 14: Specific momentum  $L_+$  for  $e = 0.11, \Lambda' = -0.001$  for different values for the Kerr parameter.

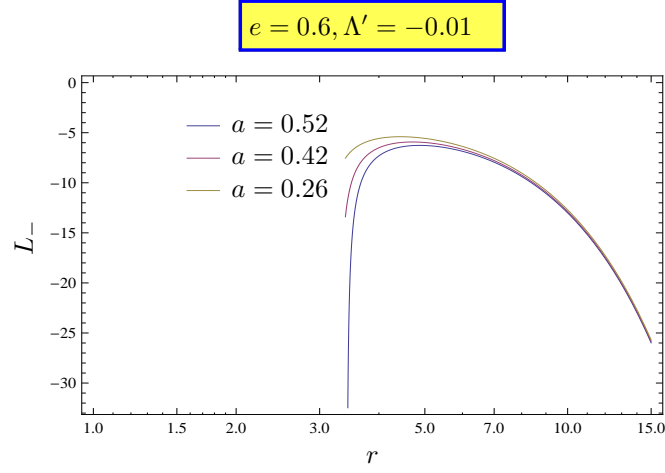


Figure 15: Specific angular momentum  $L_-$  for  $e = 0.6, \Lambda' = -0.01$  for different values for the Kerr parameter.

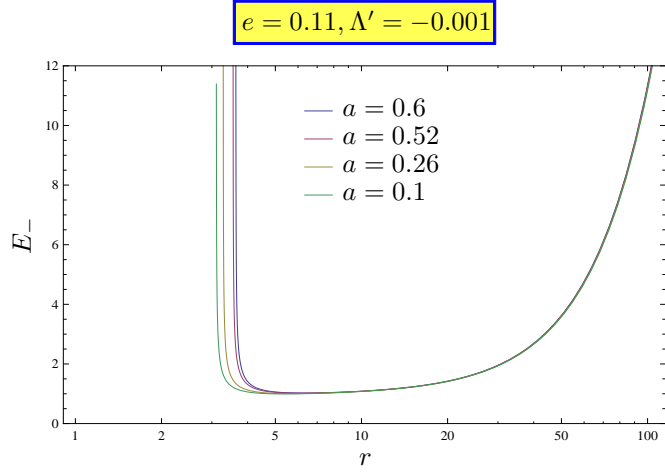


Figure 16: Specific energy  $E_-$  for  $e = 0.11, \Lambda' = -0.001$  for different values for the Kerr parameter.

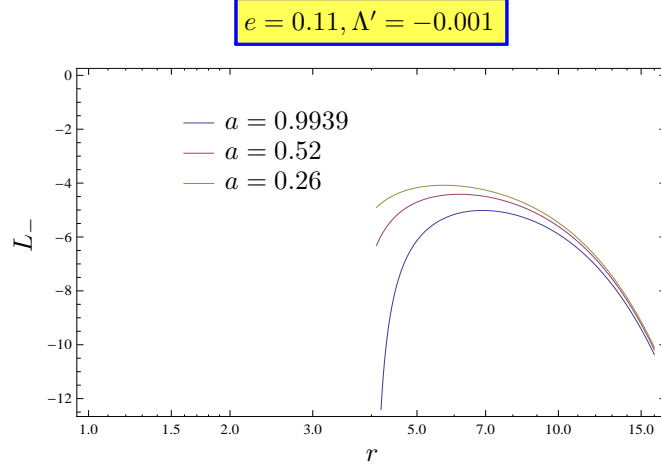


Figure 17: Specific angular momentum  $L_-$  for  $e = 0.11, \Lambda' = -0.001$  for different values for the Kerr parameter.

### 3.1 Stability of circular equatorial orbits in Kerr-Newman-de Sitter spacetime

The loci of the stable equatorial circular orbits are determined by the inequality condition:

$$\frac{d^2 R'}{dr^2} \geq 0, \quad (31)$$

which has to be satisfied simultaneously with the conditions  $R'(r) = 0$  and  $dR'/dr = 0$  determining the specific energy and specific angular momentum of the constant radius orbits. Using relations (26)-(27) we find that:

$$\begin{aligned} \frac{d^2 R'}{dr^2} \geq 0 \Leftrightarrow \\ \left\{ \left[ \pm 8ar^2 \sqrt{\frac{1}{r^3} - \Lambda' - \frac{e^2}{r^4}} r(-1 + r^3 \Lambda' + \frac{e^2}{r}) + r^2(6 - r + r^3(-15 + 4r)\Lambda') + 4e^4 + 3e^2 r(-3 + 4r^3 \Lambda') \right. \right. \\ \left. \left. + a^2(-4e^2 + r[3 + r^2 \Lambda'(1 - 4r^3 \Lambda')]) \right] 2(2e^2 + r(-3 + r \pm 2ar \sqrt{\frac{1}{r^3} - \Lambda' - \frac{e^2}{r^4}} - a^2 r \Lambda')) \right\} / \\ [2e^2 + r(-3 + r \pm 2ar \sqrt{\frac{1}{r^3} - \Lambda' - \frac{e^2}{r^4}} - a^2 r \Lambda')]^2 \geq 0. \end{aligned} \quad (32)$$



Due to reality conditions (28) we find that the radii of the stable orbits in Kerr-Newman-de Sitter spacetime are restricted by the inequality:

$$\begin{aligned} & \pm 8ar^2 \sqrt{\frac{1}{r^3} - \Lambda' - \frac{e^2}{r^4}} r(-1 + r^3 \Lambda' + \frac{e^2}{r}) + r^2(6 - r + r^3(-15 + 4r)\Lambda') + 4e^4 + 3e^2 r(-3 + 4r^3 \Lambda') \\ & + a^2(-4e^2 + r[3 + r^2 \Lambda'(1 - 4r^3 \Lambda')]) \geq 0. \end{aligned} \quad (33)$$

The marginally stable orbits can be obtained by solving the quadratic equation (embedded in (33)) for the rotational parameter a procedure that yields the relation:

$$\begin{aligned} a^2 &= a_{\text{ms}(1,2)}^2 \\ &\equiv \left\{ 128r(1 - r^3 \Lambda' - e^2/r)^3 r^2 \right. \\ &\quad - 4[-4e^2 + r(3 + r^2 \Lambda'(1 - 4r^3 \Lambda'))] \{ r^2(6 - r + r^3(-15 + 4r)\Lambda') + 4e^4 + 3e^2 r(-3 + 4r^3 \Lambda') \} \\ &\quad \pm 32[r(1 - r^3 \Lambda' - e^2/r)^3]^{1/2} r \sqrt{r^3} \\ &\quad \times \sqrt{(1 - 4\Lambda' r^3)} \sqrt{-2 + 3r - r^2 \Lambda'(6 + 10r - 15\Lambda' r^3) - 4e^4 \Lambda' + \frac{3e^2}{r}(1 + 4r^3 \Lambda') - 4e^2 + 9\Lambda' e^2 r - 12r^4 \Lambda' e^2} \Big\} \\ &\quad 4^{-1} [-4e^2 + r(3 + r^2 \Lambda'(1 - 4r^3 \Lambda'))]^{-2}. \end{aligned} \quad (34)$$

From (34) we deduce the following reality conditions :

$$\Lambda' \leq \Lambda'_{\text{ms}}(r) \equiv \frac{1}{4r^3}, \quad (35)$$

and

$$-2 + 3r - r^2 \Lambda'(6 + 10r - 15\Lambda' r^3) - 4e^4 \Lambda' + \frac{3e^2}{r}(1 + 4r^3 \Lambda') - 4e^2 + 9\Lambda' e^2 r - 12r^4 \Lambda' e^2 \geq 0 \quad (36)$$

$$\Leftrightarrow \Lambda'^2 15r^5 + \Lambda'[-r^2(6 + 10r) - 4e^4 + 12e^2 r^2 + 9e^2 r - 12r^4 e^2] - 2 + 3r + \frac{3e^2}{r} - 4e^2 \geq 0. \quad (37)$$

From (37) and the fact that  $15r^5 > 0$  we derive two more conditions:

$$\Lambda' \leq \Lambda'_{\text{ms}-} \quad \text{or} \quad \Lambda' \geq \Lambda'_{\text{ms}+}, \quad (38)$$

where  $\Lambda'_{\text{ms}\pm}$  are the two roots of the quadratic equation (37).

### 3.1.1 Stability of equatorial circular geodesics in Kerr-de Sitter spacetime

Our results in inequality (33), for zero electric charge,  $e = 0$ , give a condition<sup>4</sup> that agrees with the results in [29] and restricts the radii of the stable orbits in Kerr-de Sitter spacetime:

<sup>4</sup>We observe that for  $e = \Lambda = 0$ , (33) reduces correctly to the equation that determines the radii of marginally stable orbits in Kerr spacetime:  $r^2 - 6Mr - 3a^2 \mp 8a\sqrt{Mr} = 0$  for  $M = 1$ , [26].

$$\pm 8ar^2 \sqrt{\frac{1}{r^3} - \Lambda'(-1+r^3\Lambda') + r(6-r+r^3(-15+4r)\Lambda') + a^2(3+r^2\Lambda'(1-4r^3\Lambda'))} \geq 0. \quad (39)$$

## 4 Gravitational redshift-blueshift of emitted photons

In this section we will provide general expressions for the redshift/blueshift that emitted photons by massive particles experience while travelling along null geodesics towards an observer located far away from their source.

In general, the frequency of a photon measured by an observer with proper velocity  $U_A^\mu$  at the spacetime point  $P_A$  reads[15],[31]:

$$\omega_A = k_\mu U_A^\mu|_{P_A}, \quad (40)$$

where the index  $A$  refers to the emission ( $e$ ) and/or detection ( $d$ ) at the corresponding point  $P_A$ .

The emission frequency is defined as follows:

$$\begin{aligned} \omega_e &= k_\mu U^\mu \\ &= k_t U^t + k_r U^r + k_\theta U^\theta + k_\phi U^\phi \\ &= (k^t E - k^\phi L + g_{rr} k^r U^r + g_{\theta\theta} k^\theta U^\theta)|_e. \end{aligned} \quad (41)$$

Likewise the detected frequency is given by the expression:

$$\begin{aligned} \omega_d &= k_\mu U^\mu \\ &= (E k^t - L k^\phi + g_{rr} k^r U^r + g_{\theta\theta} k^\theta U^\theta)|_d. \end{aligned} \quad (42)$$

In producing (41),(42) we used the expressions for  $U^t$  and  $U^\phi$  in terms of the metric components and the conserved quantities  $E, L$ :

$$U^t = \frac{-E g_{\phi\phi} - L g_{t\phi}}{g_{t\phi}^2 - g_{tt} g_{\phi\phi}}, \quad (43)$$

$$U^\phi = \frac{g_{tt} L + g_{\phi t} E}{g_{t\phi}^2 - g_{tt} g_{\phi\phi}}. \quad (44)$$

Thus, the frequency shift associated to the emission and detection of photons is given by either of the following relations:

$$\begin{aligned} 1 + z &= \frac{\omega_e}{\omega_d} \\ &= \frac{(k^t E - k^\phi L + g_{rr} k^r U^r + g_{\theta\theta} k^\theta U^\theta)|_e}{(E k^t - L k^\phi + g_{rr} k^r U^r + g_{\theta\theta} k^\theta U^\theta)|_d} \\ &= \frac{(E_\gamma U^t - L_\gamma U^\phi + g_{rr} K^r U^r + g_{\theta\theta} K^\theta U^\theta)|_e}{(E_\gamma U^t - L_\gamma U^\phi + g_{rr} K^r U^r + g_{\theta\theta} K^\theta U^\theta)|_d} \end{aligned} \quad (45)$$

This is the most general expression for the redshift/blueshift that light signals emitted by massive test particles experience in their path along null geodesics towards a distant observer (ideally located near the cosmological horizon in particular or at spatial infinity assuming a zero cosmological constant).

#### 4.1 The redshift/blueshift of photons for circular and equatorial emitter/detector orbits around the Kerr-Newman-(anti) de Sitter black hole

For equatorial circular orbits  $U^r = U^\theta = 0$  thus

$$1 + z = \frac{(E_\gamma U^t - L_\gamma U^\phi)|_e}{(E_\gamma U^t - L_\gamma U^\phi)|_d} = \frac{U^t - \Phi U^\phi|_e}{U^t - \Phi U^\phi|_d} = \frac{U_e^t - \Phi_e U_e^\phi}{U_d^t - \Phi_d U_d^\phi}, \quad (46)$$

where  $\Phi = L_\gamma/E_\gamma$ . For  $\Phi = 0$ ,  $1 + z_c = \frac{U_e^t}{U_d^t}$ . Following the procedure for the Kerr black hole in [31], we consider the kinematic redshift of photons either side of the line of sight that links the Kerr-Newman-de Sitter black hole and the observer, and subtract from Eq.(46) the central value  $z_c$ . Then we obtain:

$$\begin{aligned} z_{\text{kin}} \equiv z - z_c &= \frac{U_e^t - \Phi_e U_e^\phi}{U_d^t - \Phi_d U_d^\phi} - \frac{U_e^t}{U_d^t} \\ &= \frac{\Phi_d U_d^\phi U_e^t - \Phi_e U_e^\phi U_d^t}{U_d^t U_d^t - \Phi_d U_d^\phi U_d^t}. \end{aligned} \quad (47)$$

Let us now consider photons with 4-momentum vector  $k^\mu = (k^t, k^r, k^\theta, k^\phi)$  which move along null geodesics  $k^\mu k_\mu = 0$  outside the event horizon of the Kerr-Newman-de Sitter black hole, which explicitly can be expressed as

$$\begin{aligned} 0 &= g_{tt}(k^t)^2 + 2g_{t\phi}(k^t k^\phi) + g_{\phi\phi}(k^\phi)^2 + g_{rr}(k^r)^2 \\ &\quad + g_{\theta\theta}(k^\theta)^2. \end{aligned} \quad (48)$$

$$\begin{aligned} k^t &= \frac{\Xi^2 \Delta_\theta (r^2 + a^2) [(r^2 + a^2) E_\gamma - a L_\gamma] - a \Xi^2 \Delta_r^{KN} (a E_\gamma \sin^2 \theta - L_\gamma)}{\Delta_r^{KN} \Delta_\theta \rho^2} \\ &= \frac{E_\gamma [\Xi^2 \Delta_\theta (r^2 + a^2)^2 - a^2 \sin^2 \theta \Xi^2 \Delta_r^{KN}] + L_\gamma [-a \Xi^2 \Delta_\theta (r^2 + a^2) + a \Xi^2 \Delta_r^{KN}]}{\Delta_r^{KN} \Delta_\theta \rho^2}, \end{aligned} \quad (49)$$

$$\begin{aligned} k^\phi &= \frac{-\Xi^2 \Delta_r^{KN} (a E_\gamma \sin^2 \theta - L_\gamma) + a \Xi^2 \Delta_\theta \sin^2 \theta [(r^2 + a^2) E_\gamma - a L_\gamma]}{\Delta_r^{KN} \Delta_\theta \rho^2 \sin^2 \theta} \\ &= \frac{[-\Xi^2 \Delta_r^{KN} a \sin^2 \theta + a \Xi^2 \Delta_\theta \sin^2 \theta (r^2 + a^2)] E_\gamma + L_\gamma [\Xi^2 \Delta_r^{KN} - a^2 \Xi^2 \Delta_\theta \sin^2 \theta]}{\Delta_r^{KN} \Delta_\theta \rho^2 \sin^2 \theta}, \end{aligned} \quad (50)$$

$$(k^\theta)^2 = \frac{\mathcal{Q}_\gamma \Delta_\theta + (L_\gamma - a E_\gamma) \Xi^2 \Delta_\theta - \frac{\Xi^2 (a E_\gamma \sin^2 \theta - L_\gamma)^2}{\sin^2 \theta}}{\rho^4} \quad (51)$$

We must take into account the bending of light from the rotating and charged Kerr-Newman-(anti) de Sitter black hole. From (47) it follows that the apparent impact parameter must be maximised. The apparent impact factor  $\Phi_\gamma \equiv L_\gamma/E_\gamma$  can be obtained from the expression  $k^\mu k_\mu = 0$ <sup>5</sup> as follows:

$$\begin{aligned} k^\mu k_\mu = 0 &\Leftrightarrow k^t k_t + k^\phi k_\phi = 0 \\ &\Leftrightarrow \left[ \frac{E_\gamma g_{\phi\phi} + g_{t\phi} L_\gamma}{g_{t\phi}^2 - g_{\phi\phi} g_{tt}} \right] (-E_\gamma) + \left[ \frac{-L_\gamma g_{tt} - E_\gamma g_{\phi t}}{g_{t\phi}^2 - g_{\phi\phi} g_{tt}} \right] L_\gamma = 0 \\ &\Leftrightarrow g_{\phi\phi} + 2g_{t\phi} \Phi_\gamma + \Phi_\gamma^2 g_{tt} = 0 \end{aligned} \quad (52)$$

Solving the quadratic equation we obtain:

$$\Phi_\gamma^\pm = \frac{-g_{\phi t} \pm \sqrt{g_{t\phi}^2 - g_{\phi\phi} g_{tt}}}{g_{tt}} = \frac{a(\Delta_r^{KN} - (r^2 + a^2)) \pm r^2 \sqrt{\Delta_r^{KN}}}{\Delta_r^{KN} - a^2}. \quad (53)$$

where we got two values,  $\Phi_\gamma^+$  and  $\Phi_\gamma^-$  (either evaluated at the emitter or detector position, since this quantity is preserved along the null geodesic photon orbits, i.e.,  $\Phi_e = \Phi_d$ ) that give rise to two different shifts respectively,  $z_1$  and  $z_2$  of the emitted photons corresponding to a receding and to an approaching object with respect to a far away positioned observer:

$$z_1 = \frac{\Phi_d^- U_d^\phi U_e^t - \Phi_e^- U_e^\phi U_d^t}{U_d^t (U_d^t - \Phi_d^- U_d^\phi)}, \quad (54)$$

$$z_2 = \frac{\Phi_d^+ U_d^\phi U_e^t - \Phi_e^+ U_e^\phi U_d^t}{U_d^t (U_d^t - \Phi_d^+ U_d^\phi)} \quad (55)$$

In general the two values  $z_1$  and  $z_2$  differ from each other due to light bending experienced by the emitted photons and the differential rotation experienced by the detector as encoded in  $U_d^\phi$  and  $U_d^t$  components of the four-velocity<sup>6</sup>.

In order to get a closed analytic expression for the gravitational redshift/blueshift experienced by the emitted photons we shall express the required quantities in terms of the Kerr-Newman-(anti) de Sitter metric. Thus, the  $U^\phi$  and  $U^t$  components of the four-velocity for circular equatorial orbits read:

$$U^t(r, \pi/2) = \frac{-(\Delta_r^{KN} a^2 - (r^2 + a^2)^2)E - L(-a(\Delta_r^{KN} - (r^2 + a^2)))}{\frac{\Xi^2 r^2 \Delta_r^{KN}}{\Xi^4}}, \quad (56)$$

$$U^\phi(r, \theta = \pi/2) = \frac{\Xi^2(\Delta_r^{KN} - a^2)L + E\Xi^2(-a(\Delta_r^{KN} - (r^2 + a^2)))}{r^2 \Delta_r^{KN}}. \quad (57)$$

<sup>5</sup>Taking into account that  $k^r = 0$  and  $k^\theta = 0$ .

<sup>6</sup>The second term in the denominator in equations (54)-(55) encodes the contribution of the movement of the detector's frame [31]. If this quantity is negligible in comparison to the contribution stemming from the  $U_d^t$  component then the detector can be considered static at spatial infinity.

Substituting the expressions (26)-(27) for  $E_{\pm}$  and  $L_{\pm}$  into  $U^t(r, \pi/2), U^{\phi}(r, \pi/2)$  we finally obtain remarkable novel expressions for these four-velocity components in Kerr-Newman-(anti) de Sitter spacetime:

$$U^t(r, \pi/2) = \frac{(r^2 \pm a\sqrt{-e^2 + r^4(\frac{1}{r^3} - \Lambda')}) \Xi^2}{r\sqrt{2e^2 + r(r-3) - r^2a^2\Lambda' \pm 2a\sqrt{-e^2 + r^4(\frac{1}{r^3} - \Lambda')}}}, \quad (58)$$

$$U^{\phi}(r, \pi/2) = \frac{\pm\sqrt{-e^2 + r^4(\frac{1}{r^3} - \Lambda')} \Xi^2}{r\sqrt{2e^2 + r(r-3) - r^2a^2\Lambda' \pm 2a\sqrt{-e^2 + r^4(\frac{1}{r^3} - \Lambda')}}}. \quad (59)$$

We now compute the angular velocity  $\Omega$ :

$$\Omega \equiv \frac{d\phi}{dt} = \frac{1}{a \pm \frac{r^{3/2}}{\sqrt{1 - \Lambda' r^3 - \frac{e^2}{r}}}}. \quad (60)$$

In terms of the angular velocities the quantities  $z_1, z_2$  read as follows:

$$\begin{aligned} z_1 &= \frac{\Phi_d^- \Omega_d U_e^t - \Phi_e^- U_d^{\phi}}{U_d^t - \Phi_d^- U_d^{\phi}} \\ &= \frac{U_e^t [\Phi_d^- \Omega_d - \Phi_e^- \Omega_e]}{U_d^t (1 - \Phi_d^- \Omega_d)}, \end{aligned} \quad (61)$$

$$\begin{aligned} z_2 &= \frac{\Phi_d^+ \Omega_d U_e^t - \Phi_e^+ U_d^{\phi}}{U_d^t - \Phi_d^+ U_d^{\phi}} \\ &= \frac{\Phi_d^+ \Omega_d U_e^t - \Phi_e^+ U_d^{\phi}}{U_d^t (1 - \Phi_d^+ \Omega_d)} \\ &= \frac{U_e^t [\Phi_d^+ \Omega_d - \Phi_e^+ \Omega_e]}{U_d^t (1 - \Phi_d^+ \Omega_d)}. \end{aligned} \quad (62)$$

Thus for the Kerr-Newman-(anti) de Sitter black hole we can write for the redshift and blueshift, respectively:

$$\begin{aligned} z_{\text{red}} &= \frac{\Omega_d \Phi_d^- - \Phi_e^- \Omega_e}{1 - \Phi_d^- \Omega_d} \frac{[r_e^{3/2} \pm a\sqrt{-e^2/r_e + r_e^3(\frac{1}{r_e^3} - \Lambda')}]}{r_e^{3/4} \sqrt{\frac{2e^2}{r_e^{1/2}} + r_e^{3/2} - 3\sqrt{r_e} - r_e^{3/2}a^2\Lambda' \pm 2a\sqrt{-e^2/r_e + r_e^3(\frac{1}{r_e^3} - \Lambda')}}} \\ &\quad \times \frac{r_d^{3/4} \sqrt{\frac{2e^2}{r_d^{1/2}} + r_d^{3/2} - 3\sqrt{r_d} - r_d^{3/2}a^2\Lambda' \pm 2a\sqrt{-e^2/r_d + r_d^3(\frac{1}{r_d^3} - \Lambda')}}}{r_d^{3/2} \pm a\sqrt{-e^2/r_d + r_d^3(\frac{1}{r_d^3} - \Lambda')}}}, \end{aligned} \quad (63)$$

$$\begin{aligned}
z_{\text{blue}} = & \frac{\Omega_d \Phi_d^+ - \Phi_e^+ \Omega_e}{1 - \Phi_d^+ \Omega_d} \frac{[r_e^{3/2} \pm a \sqrt{-e^2/r_e + r_e^3 \left(\frac{1}{r_e^3} - \Lambda'\right)}]}{r_e^{3/4} \sqrt{\frac{2e^2}{r_e^{1/2}} + r_e^{3/2} - 3\sqrt{r_e} - r_e^{3/2} a^2 \Lambda' \pm 2a \sqrt{-e^2/r_e + r_e^3 \left(\frac{1}{r_e^3} - \Lambda'\right)}}} \\
& \times \frac{r_d^{3/4} \sqrt{\frac{2e^2}{r_d^{1/2}} + r_d^{3/2} - 3\sqrt{r_d} - r_d^{3/2} a^2 \Lambda' \pm 2a \sqrt{-e^2/r_d + r_d^3 \left(\frac{1}{r_d^3} - \Lambda'\right)}}}{r_d^{3/2} \pm a \sqrt{-e^2/r_d + r_d^3 \left(\frac{1}{r_d^3} - \Lambda'\right)}}, \tag{64}
\end{aligned}$$

where now  $r_e$  and  $r_d$  stand for the radius of the emitter's and detector's orbits, respectively. These elegant and novel expressions can be written in terms of the physical parameters of the Kerr-Newman-(anti) de Sitter black hole and the detector radius,  $r_d$ , as follows:

$$\begin{aligned}
z_{\text{red}} = & \frac{r_d^{3/4} \sqrt{\frac{2e^2}{r_d^{1/2}} + r_d^{3/2} - 3\sqrt{r_d} - r_d^{3/2} a^2 \Lambda' \pm 2a \sqrt{-e^2/r_d + r_d^3 \left(\frac{1}{r_d^3} - \Lambda'\right)}}}{r_e^{3/4} \sqrt{\frac{2e^2}{r_e^{1/2}} + r_e^{3/2} - 3\sqrt{r_e} - r_e^{3/2} a^2 \Lambda' \pm 2a \sqrt{-e^2/r_e + r_e^3 \left(\frac{1}{r_e^3} - \Lambda'\right)}}} \\
& \times \frac{\left(a(-\Lambda' r_e^2(r_e^2 + a^2) - 2r_e + e^2) - r_e^2 \sqrt{\Delta_r^{KN}(r_e)}\right) (\pm [r_e^{3/2} \sqrt{1 - \Lambda' r_d^3 - \frac{e^2}{r_d}} - r_d^{3/2} \sqrt{1 - \Lambda' r_e^3 - \frac{e^2}{r_e}}])}{(r_d^{3/2} \pm a \sqrt{1 - \Lambda' r_d^3 - \frac{e^2}{r_d}}) [(\Delta_r^{KN}(r_e) - a^2) r_d^{3/2} + (a r_e^2 + r_e^2 \sqrt{\Delta_r^{KN}(r_e)}) (\pm \sqrt{1 - \Lambda' r_d^3 - \frac{e^2}{r_d}})]} \tag{65}
\end{aligned}$$

$$\begin{aligned}
z_{\text{blue}} = & \frac{r_d^{3/4} \sqrt{\frac{2e^2}{r_d^{1/2}} + r_d^{3/2} - 3\sqrt{r_d} - r_d^{3/2} a^2 \Lambda' \pm 2a \sqrt{-e^2/r_d + r_d^3 \left(\frac{1}{r_d^3} - \Lambda'\right)}}}{r_e^{3/4} \sqrt{\frac{2e^2}{r_e^{1/2}} + r_e^{3/2} - 3\sqrt{r_e} - r_e^{3/2} a^2 \Lambda' \pm 2a \sqrt{-e^2/r_e + r_e^3 \left(\frac{1}{r_e^3} - \Lambda'\right)}}} \\
& \times \frac{\left(a(-\Lambda' r_e^2(r_e^2 + a^2) - 2r_e + e^2) + r_e^2 \sqrt{\Delta_r^{KN}(r_e)}\right) (\pm [r_e^{3/2} \sqrt{1 - \Lambda' r_d^3 - \frac{e^2}{r_d}} - r_d^{3/2} \sqrt{1 - \Lambda' r_e^3 - \frac{e^2}{r_e}}])}{(r_d^{3/2} \pm a \sqrt{1 - \Lambda' r_d^3 - \frac{e^2}{r_d}}) [(\Delta_r^{KN}(r_e) - a^2) r_d^{3/2} + (a r_e^2 - r_e^2 \sqrt{\Delta_r^{KN}(r_e)}) (\pm \sqrt{1 - \Lambda' r_d^3 - \frac{e^2}{r_d}})]}, \tag{66}
\end{aligned}$$

where we define:

$$\Delta_r^{KN}(r_e) := (1 - \Lambda' r_e^2)(r_e^2 + a^2) - 2r_e + e^2 \tag{67}$$

and we have made use of the relation  $\Phi_e = \Phi_d$ . The remarkable closed form analytic expressions for the frequency shifts we obtained in eqns.(65)-(66), constitute a new result in the theory of General Relativity, in which all the physical parameters of the exact theory enter on an equal footing.

#### 4.1.1 Redshift/blueshift for circular equatorial orbits in Kerr-de Sitter spacetime

For zero electric charge,  $e = 0$ , eqns.(65)-(66) reduce to:

$$z_{\text{red}} = \frac{r_d^{3/4} \sqrt{r_d^{3/2} - 3\sqrt{r_d} - r_d^{3/2} a^2 \Lambda' \pm 2a \sqrt{r_d^3 (\frac{1}{r_d^3} - \Lambda')}}}{r_e^{3/4} \sqrt{r_e^{3/2} - 3\sqrt{r_e} - r_e^{3/2} a^2 \Lambda' \pm 2a \sqrt{r_e^3 (\frac{1}{r_e^3} - \Lambda')}}} \times \frac{[a(-\Lambda' r_e^2 (r_e^2 + a^2) - 2r_e) - r_e^2 \sqrt{\Delta_r(r_e)}](\pm [r_e^{3/2} \sqrt{1 - \Lambda' r_d^3} - r_d^{3/2} \sqrt{1 - \Lambda' r_e^3}])}{(r_d^{3/2} \pm a \sqrt{1 - \Lambda' r_d^3})[(\Delta_r(r_e) - a^2) r_d^{3/2} + (a r_e^2 + r_e^2 \sqrt{\Delta_r(r_e)}) (\pm \sqrt{1 - \Lambda' r_d^3})]}, \quad (68)$$

$$z_{\text{blue}} = \frac{r_d^{3/4} \sqrt{r_d^{3/2} - 3\sqrt{r_d} - r_d^{3/2} a^2 \Lambda' \pm 2a \sqrt{r_d^3 (\frac{1}{r_d^3} - \Lambda')}}}{r_e^{3/4} \sqrt{r_e^{3/2} - 3\sqrt{r_e} - r_e^{3/2} a^2 \Lambda' \pm 2a \sqrt{r_e^3 (\frac{1}{r_e^3} - \Lambda')}}} \times \frac{[a(-\Lambda' r_e^2 (r_e^2 + a^2) - 2r_e) + r_e^2 \sqrt{\Delta_r(r_e)}](\pm [r_e^{3/2} \sqrt{1 - \Lambda' r_d^3} - r_d^{3/2} \sqrt{1 - \Lambda' r_e^3}])}{(r_d^{3/2} \pm a \sqrt{1 - \Lambda' r_d^3})[(\Delta_r(r_e) - a^2) r_d^{3/2} + (a r_e^2 - r_e^2 \sqrt{\Delta_r(r_e)}) (\pm \sqrt{1 - \Lambda' r_d^3})]}. \quad (69)$$

In the particular case when the detector is located far away from the source and the condition is fulfilled:  $r_d \gg M \geq a$ , the redshift and blueshift respectively take the form:

$$z_{\text{red}} = \frac{\sqrt{1 - a^2 \Lambda'} [a(\Lambda' r_e^2 (r_e^2 + a^2) + 2r_e) + r_e^2 \sqrt{\Delta_r(r_e)}] (\pm \sqrt{1 - \Lambda' r_e^3})}{r_e^{3/4} \sqrt{r_e^{3/2} - 3\sqrt{r_e} - r_e^{3/2} a^2 \Lambda' \pm 2a \sqrt{r_e^3 (\frac{1}{r_e^3} - \Lambda')}} [\Delta_r(r_e) - a^2]}, \quad (70)$$

$$z_{\text{blue}} = \frac{\sqrt{1 - a^2 \Lambda'} [a(\Lambda' r_e^2 (r_e^2 + a^2) + 2r_e) - r_e^2 \sqrt{\Delta_r(r_e)}] (\pm \sqrt{1 - \Lambda' r_e^3})}{r_e^{3/4} \sqrt{r_e^{3/2} - 3\sqrt{r_e} - r_e^{3/2} a^2 \Lambda' \pm 2a \sqrt{r_e^3 (\frac{1}{r_e^3} - \Lambda')}} [\Delta_r(r_e) - a^2]}. \quad (71)$$

The frequency shifts (70)-(71) are plotted in Figs.(18)-(19) for different values of the spin of the central black hole and for positive cosmological constant for the corotating case. As the radius increases,  $z_{\text{red}} \rightarrow -z_{\text{blue}}$ .

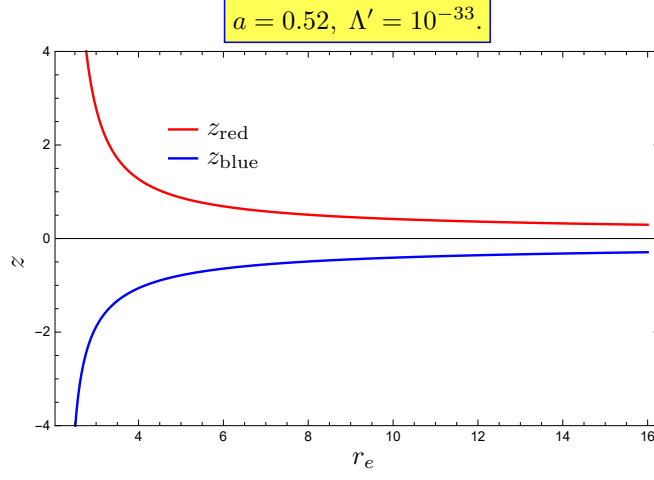


Figure 18: The functions  $z_{\text{red}}, z_{\text{blue}}$  as functions of radius  $r_e$ . The spin of the Kerr-Newman-de Sitter black hole was chosen as  $a = 0.52$  and the dimensionless cosmological parameter as  $\Lambda' = 10^{-33}$ .

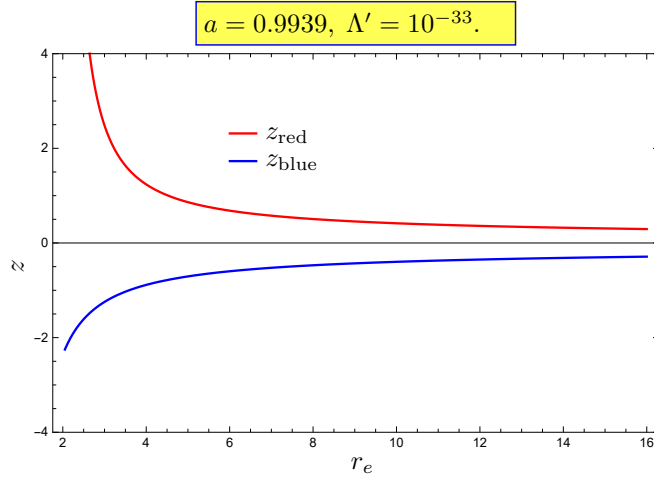


Figure 19: The functions  $z_{\text{red}}, z_{\text{blue}}$  as functions of radius  $r_e$ . The spin of the Kerr-Newman-de Sitter black hole was chosen as  $a = 0.9939$  and the dimensionless cosmological parameter as  $\Lambda' = 10^{-33}$ .



## 5 More general orbits for rotating charged black holes

### 5.1 Spherical orbits in Kerr-Newman spacetime

#### 5.1.1 Frame-dragging for timelike spherical orbits

Assuming  $\Lambda = 0$  we derive from (8) and (11) the following equation:

$$\frac{d\phi}{d\theta} = \frac{\frac{aP}{\Delta^{KN}} - aE + L/\sin^2\theta}{\sqrt{Q - \frac{L^2 \cos^2\theta}{\sin^2\theta} + a^2 \cos^2\theta(E^2 - 1)}}. \quad (72)$$

In (72)  $\Delta^{KN} := r^2 + a^2 + e^2 - 2Mr$ .<sup>7</sup> Using the variable  $z = \cos^2\theta$ ,  $-\frac{1}{2}\frac{dz}{\sqrt{z}}\frac{1}{\sqrt{1-z}} = \text{sgn}(\pi/2 - \theta)d\theta$  we will determine for the *first time* in closed analytic form the amount of frame-dragging for timelike spherical orbits in the Kerr-Newman spacetime<sup>8</sup>.

Thus for instance, expressed in terms of the new variable :

$$\begin{aligned} \frac{L}{\sin^2\theta} \frac{d\theta}{\sqrt{\Theta}} &= \frac{L}{1-z} \left(-\frac{1}{2}\right) \frac{dz}{\sqrt{z}} \frac{1}{\sqrt{\alpha z^2 - (\alpha + \beta)z + Q}} \\ &= \frac{L}{1-z} \left(-\frac{1}{2}\right) \frac{dz}{\sqrt{z}} \frac{1}{|a|\sqrt{1-E^2}} \frac{1}{\sqrt{(z-z_+)(z-z_-)}}, \end{aligned} \quad (73)$$

where  $\alpha = a^2(1-E^2)$ ,  $\beta = L^2 + Q$ . The range of  $z$  for which the motion takes place includes the equatorial value,  $z = 0$ :

$$0 \leq z \leq z_-. \quad (74)$$

We will prove first the following exact result:

#### Proposition 1

$$\begin{aligned} &\int_0^{z_-} \frac{L}{1-z} \left(-\frac{1}{2}\right) \frac{dz}{\sqrt{z}} \frac{1}{|a|\sqrt{1-E^2}} \frac{1}{\sqrt{(z-z_+)(z-z_-)}} \\ &= -\frac{L}{|a|\sqrt{1-E^2}} \frac{\pi}{2} (1-z_-)^{-1} (z_+ - z_-)^{-1/2} F_1\left(\frac{1}{2}, 1, \frac{1}{2}, 1, \frac{z_-}{z_- - 1}, \frac{z_-}{z_- - z_+}\right) \\ &= -\frac{L}{|a|\sqrt{1-E^2}} \frac{\pi}{2} z_+^{-1/2} F_1\left(\frac{1}{2}, \frac{1}{2}, 1, 1, \frac{z_-}{z_+}, z_-\right). \end{aligned} \quad (75)$$

**Proof.** We compute first the integral:

$$\int_{z_j}^{z_-} \frac{L}{1-z} \left(-\frac{1}{2}\right) \frac{dz}{\sqrt{z}} \frac{1}{|a|\sqrt{1-E^2}} \frac{1}{\sqrt{(z-z_+)(z-z_-)}}. \quad (76)$$

<sup>7</sup>When we set  $M = 1$ ,  $\Delta^{KN} = r^2 + a^2 + e^2 - 2r$ .

<sup>8</sup>We should mention at this point the extreme black hole solutions for spherical timelike non-polar geodesics in Kerr-Newman spacetime obtained in [34] in terms of formal integrals.

Applying the transformation  $z = z_- + \xi^2(z_j - z_-)$  in (76) we obtain

$$\begin{aligned}
& \int_{z_j}^{z_-} \frac{L}{1-z} \left(-\frac{1}{2}\right) \frac{dz}{\sqrt{z}} \frac{1}{|a|\sqrt{1-E^2}} \frac{1}{\sqrt{(z-z_+)(z-z_-)}} \\
&= \frac{-L}{2|a|\sqrt{1-E^2}} \frac{z_- - z_j}{(1-z_-)} \frac{1}{\sqrt{z_-}\sqrt{z_- - z_+}\sqrt{z_j - z_-}} \int_0^1 \frac{dx}{[1-x\left(\frac{z_j-z_-}{1-z_-}\right)]} \frac{1}{\sqrt{1-x\frac{z_- - z_j}{z_- - z_+}}} \frac{1}{\sqrt{x}} \frac{1}{\sqrt{1-x\frac{z_- - z_j}{z_-}}} \\
&= \frac{-L}{2|a|\sqrt{1-E^2}} \frac{z_- - z_j}{(1-z_-)} \frac{1}{\sqrt{z_-}\sqrt{z_- - z_+}\sqrt{z_j - z_-}} \\
&\times \frac{\Gamma(\frac{1}{2})\Gamma(1)}{\Gamma(\frac{3}{2})} F_D\left(\frac{1}{2}, 1, \frac{1}{2}, \frac{1}{2}, \frac{3}{2}, \frac{z_j - z_-}{1-z_-}, \frac{z_- - z_j}{z_-}, \frac{z_- - z_j}{z_- - z_+}\right), \tag{77}
\end{aligned}$$

where  $x \equiv \xi^2$ . Setting  $z_j = 0$  yields:

$$\begin{aligned}
& \int_0^{z_-} \frac{L}{1-z} \left(-\frac{1}{2}\right) \frac{dz}{\sqrt{z}} \frac{1}{|a|\sqrt{1-E^2}} \frac{1}{\sqrt{(z-z_+)(z-z_-)}} \\
&= \frac{-L}{2|a|\sqrt{1-E^2}} (1-z_-)^{-1} (z_+ - z_-)^{-1/2} \frac{\Gamma(\frac{1}{2})\Gamma(1)}{\Gamma(\frac{3}{2})} F_D\left(\frac{1}{2}, 1, \frac{1}{2}, \frac{1}{2}, \frac{3}{2}, \frac{-z_-}{1-z_-}, 1, \frac{z_-}{z_- - z_+}\right) \\
&= \frac{-L}{2|a|\sqrt{1-E^2}} (1-z_-)^{-1} (z_+ - z_-)^{-1/2} \frac{\Gamma(1/2)^2\Gamma(\frac{3}{2})}{\Gamma(\frac{3}{2})} F_1\left(\frac{1}{2}, 1, \frac{1}{2}, 1, \frac{-z_-}{1-z_-}, \frac{z_-}{z_- - z_+}\right) \\
&= \frac{-L}{2|a|\sqrt{1-E^2}} z_+^{-1/2} \pi F_1\left(\frac{1}{2}, \frac{1}{2}, 1, 1, \frac{z_-}{z_+}, z_-\right). \tag{78}
\end{aligned}$$

■

For producing the result in the last line of equation (78), we used the following transformation property of Appell's hypergeometric function  $F_1$ :

**Lemma 2**

$$\begin{aligned}
& y^{1+\beta-\gamma} (1-y)^{\gamma-\alpha-1} (x-y)^{-\beta} F_1\left(1-\beta', \beta, 1+\alpha-\gamma, 2+\beta-\gamma, \frac{y}{y-x}, \frac{y}{y-1}\right) \\
&= y^{1+\beta-\gamma} x^{-\beta} F_1\left(1+\beta+\beta'-\gamma, \beta, 1+\alpha-\gamma, 2+\beta-\gamma, \frac{y}{x}, y\right). \tag{79}
\end{aligned}$$

On the other hand we compute analytically the second integral that contributes to frame-dragging and we obtain:

**Proposition 3**

$$\begin{aligned}
& \int_0^{z_-} \frac{\frac{aP}{\Delta^{KN}} - aE}{\sqrt{\Theta'}} d\theta \\
&= \left(\frac{aP}{\Delta^{KN}} - aE\right) \frac{1}{|a|\sqrt{1-E^2}} \left(-\frac{1}{2}\right) \frac{\Gamma(\frac{1}{2})\Gamma(\frac{1}{2})}{\sqrt{z_+ - z_-}} F\left(\frac{1}{2}, \frac{1}{2}, 1, -\frac{z_-}{z_+ - z_-}\right) \\
&= \left(\frac{aP}{\Delta^{KN}} - aE\right) \frac{1}{|a|\sqrt{1-E^2}} \left(-\frac{\pi}{2}\right) \frac{1}{\sqrt{z_+}} F\left(\frac{1}{2}, \frac{1}{2}, 1, \frac{z_-}{z_+}\right). \tag{80}
\end{aligned}$$

We thus obtain the following result in closed analytic form for the amount of frame-dragging that a timelike spherical orbit in Kerr-Newman spacetime undergoes.

**Theorem 4** *As  $\theta$  goes through a quarter of a complete oscillation we obtain the change in azimuth  $\phi$ ,  $\Delta\phi^{\text{GTR}}$ :*

$$\begin{aligned}\Delta\phi^{\text{GTR}} = & -\frac{L}{|a|\sqrt{1-E^2}} \frac{\pi}{2} z_+^{-1/2} F_1\left(\frac{1}{2}, \frac{1}{2}, 1, 1, \frac{z_-}{z_+}, z_-\right) \\ & + \left(\frac{aP}{\Delta^{KN}} - aE\right) \frac{1}{|a|\sqrt{1-E^2}} \left(-\frac{\pi}{2}\right) \frac{1}{\sqrt{z_+}} F\left(\frac{1}{2}, \frac{1}{2}, 1, \frac{z_-}{z_+}\right).\end{aligned}\quad (81)$$

## 5.2 Periods

Squaring the geodesic differential equation for the polar variable (11) (for  $\Lambda = 0$ ), multiplying by the term  $\cos^2\theta \sin^2\theta$ , and making the change to the variable  $z$ , yields the following differential equation for the proper polar period:

$$d\tau_\theta = \frac{(r^2 + a^2 z) dz}{2\sqrt{z}\sqrt{a^2(1-E^2)z^2 + (-a^2(1-E^2) - L^2 - Q)z + Q}} \quad (82)$$

Finally our closed form analytic computation for the proper polar period yields:

**Proposition 5**

$$\begin{aligned}\tau_\theta = & 4 \left[ \frac{r^2}{|a|\sqrt{1-E^2}} \frac{\pi}{2} \frac{1}{\sqrt{z_+}} F\left(\frac{1}{2}, \frac{1}{2}, 1, \frac{z_-}{z_+}\right) \right. \\ & - \frac{a^2}{2|a|\sqrt{1-E^2}} \frac{1}{\sqrt{z_+}} \Gamma\left(\frac{1}{2}\right) \Gamma\left(\frac{1}{2}\right) F\left(\frac{1}{2}, -\frac{1}{2}, 1, \frac{z_-}{z_+}\right) \\ & \left. - \frac{z_+ a^2}{2|a|\sqrt{1-E^2}} \frac{\pi}{2} \frac{1}{\sqrt{z_+}} F\left(\frac{1}{2}, \frac{1}{2}, 1, \frac{z_-}{z_+}\right) \right].\end{aligned}\quad (83)$$

**Proof.** We compute first:

$$\begin{aligned}& \int_0^{z_-} \frac{r^2 dz}{2|a|\sqrt{1-E^2}} \frac{1}{\sqrt{z}\sqrt{(z-z_-)(z-z_+)}} \\ &= \frac{r^2}{2|a|\sqrt{1-E^2}} F\left(\frac{1}{2}, \frac{1}{2}, 1, \frac{-z_-}{z_+ - z_-}\right) \Gamma\left(\frac{1}{2}\right) \Gamma\left(\frac{1}{2}\right) \frac{1}{\sqrt{z_+ - z_-}} \\ &= \frac{r^2}{2|a|\sqrt{1-E^2}} \frac{\pi}{2} \frac{1}{\sqrt{z_+}} F\left(\frac{1}{2}, \frac{1}{2}, 1, \frac{z_-}{z_+}\right).\end{aligned}\quad (84)$$

We write:

$$\int_{z_j}^{z_-} \frac{a^2 z dz}{2|a|\sqrt{1-E^2} \sqrt{z}\sqrt{(z-z_+)(z-z_-)}} = \int_{z_j}^{z_-} \frac{a^2(z-z_+ + z_+) dz}{2|a|\sqrt{1-E^2} \sqrt{z}\sqrt{(z-z_+)(z-z_-)}} \quad (85)$$

Applying the change of variables:  $z = z_- + \xi^2(z_j - z_-)$  we compute the term:

$$\begin{aligned}
& \int_{z_j}^{z_-} \frac{a^2(z - z_+)dz}{2|a|\sqrt{1-E^2}\sqrt{z}\sqrt{(z-z_+)(z-z_-)}} \\
&= \frac{a^2(z_j - z_-)}{2|a|\sqrt{1-E^2}} \int_1^0 \frac{2\xi d\xi [z_- - z_+ + \xi^2(z_j - z_-)]}{\sqrt{z_-}\sqrt{z_+ - z_-}\sqrt{z_- - z_j}\sqrt{1 - \frac{\xi^2(z_- - z_j)}{z_- - z_+}}\sqrt{\xi^2}\sqrt{1 - \frac{\xi^2(z_- - z_j)}{z_-}}} \\
&= \frac{a^2}{2|a|\sqrt{1-E^2}} \frac{(z_+ - z_-)(z_j - z_-)}{\sqrt{z_-}(z_- - z_+)(z_j - z_-)} \int_0^1 \frac{2\xi d\xi \left[1 - \frac{\xi^2(z_- - z_j)}{z_- - z_+}\right]^{1/2}}{\sqrt{1 - \frac{\xi^2(z_- - z_j)}{z_-}}\sqrt{\xi^2}} \\
&= \frac{a^2}{2|a|\sqrt{1-E^2}} \frac{(z_+ - z_-)(z_j - z_-)}{\sqrt{z_-}(z_- - z_+)(z_j - z_-)} \int_0^1 \frac{dx \left[1 - \frac{x(z_- - z_j)}{z_- - z_+}\right]^{1/2}}{\sqrt{1 - \frac{x(z_- - z_j)}{z_-}}\sqrt{x}} \\
&= \frac{a^2}{2|a|\sqrt{1-E^2}} \frac{(z_+ - z_-)(z_j - z_-)}{\sqrt{z_-}(z_- - z_+)(z_j - z_-)} F_1\left(\frac{1}{2}, -\frac{1}{2}, \frac{1}{2}, \frac{3}{2}, \frac{z_- - z_j}{z_- - z_+}, \frac{z_- - z_j}{z_-}\right) \frac{\Gamma(\frac{1}{2})\Gamma(1)}{\Gamma(\frac{3}{2})} \\
&\quad (86)
\end{aligned}$$

Setting  $z_j = 0$  in the expression which involves Appell's hypergeometric function  $F_1$  yields:

$$\begin{aligned}
& \int_0^{z_-} \frac{a^2(z - z_+)dz}{2|a|\sqrt{1-E^2}\sqrt{z}\sqrt{(z-z_+)(z-z_-)}} \\
&= \frac{-a^2}{2|a|} \frac{1}{\sqrt{1-E^2}} \frac{(z_+ - z_-)}{\sqrt{z_+ - z_-}} \frac{\Gamma(\frac{1}{2})}{\Gamma(\frac{3}{2})} \frac{\Gamma(\frac{3}{2})}{\Gamma(\frac{3}{2} - \frac{1}{2})} \frac{\Gamma(\frac{3}{2} - \frac{1}{2} - \frac{1}{2})}{\Gamma(\frac{3}{2} - \frac{1}{2})} F\left(\frac{1}{2}, -\frac{1}{2}, 1, \frac{-z_-}{z_+ - z_-}\right) \\
&\quad (87)
\end{aligned}$$

■

### 5.3 Spherical orbits in Kerr-Newman-(anti) de Sitter space-time

From (8) and (11) we derive the equation :

$$\begin{aligned}
\frac{d\phi}{d\theta} &= \frac{a\Xi^2}{\Delta_r^{\text{KN}}} \frac{[(r^2 + a^2)E - aL]}{\sqrt{\Theta'}} - \frac{\Xi^2}{(1 + \frac{a^2\Lambda}{3}\cos^2\theta)(\sin^2\theta)} \frac{aE\sin^2\theta - L}{\sqrt{\Theta'}} \\
&= \frac{a\Xi^2}{\Delta_r^{\text{KN}}} \frac{[(r^2 + a^2)E - aL]}{\sqrt{\Theta'}} - \frac{\Xi^2}{(1 + \frac{a^2\Lambda}{3}z)(1-z)} \frac{aE(1-z) - L}{\sqrt{\Theta'}}. \quad (88)
\end{aligned}$$

Using the variable  $z$  we obtain the following novel exact result in closed analytic form for the amount of frame-dragging that a timelike spherical orbit in Kerr-Newman-(anti)de Sitter spacetime undergoes. As  $\theta$  goes through a quarter of a complete oscillation we obtain the change in azimuth  $\phi$ ,  $\Delta\phi^{\text{GTR}}$  in terms

of Lauricella's  $F_D$  and Appell's  $F_1$  multivariable generalised hypergeometric functions:

$$\begin{aligned}\Delta\phi_\Lambda^{\text{GTR}} = & \frac{a\Xi^2}{\Delta_r^{\text{KN}}} \frac{[(r^2 + a^2)E - aL]}{\sqrt{z_+ - z_-}\sqrt{z_- - z_\Lambda}} \frac{\Gamma^2\left(\frac{1}{2}\right)}{-2\sqrt{a^4\frac{\Lambda}{4}}} F_1\left(\frac{1}{2}, \frac{1}{2}, \frac{1}{2}, 1, \frac{z_-}{z_- - z_+}, \frac{z_-}{z_- - z_\Lambda}\right) \\ & + \frac{H\Xi^2 aE}{2\sqrt{\frac{a^4\Lambda}{3}}} \Gamma^2\left(\frac{1}{2}\right) F_D\left(\frac{1}{2}, \frac{1}{2}, \frac{1}{2}, 1, \frac{3}{2}, \frac{z_-}{z_- - z_+}, \frac{z_-}{z_- - z_\Lambda}, -\eta\right) \\ & + \frac{-HL\Xi^2}{2\sqrt{\frac{a^4\Lambda}{3}}} \frac{\Gamma^2\left(\frac{1}{2}\right)}{1 - z_-} F_D\left(\frac{1}{2}, \frac{1}{2}, \frac{1}{2}, 1, 1, \frac{3}{2}, \frac{z_-}{z_- - z_+}, \frac{z_-}{z_- - z_\Lambda}, -\eta, \frac{-z_-}{1 - z_-}\right),\end{aligned}\tag{89}$$

where we define:

$$\begin{aligned}H &\equiv \frac{1}{\sqrt{z_+ - z_-}\sqrt{z_- - z_\Lambda}} \frac{1}{\left(1 + \frac{a^2\Lambda z_-}{3}\right)} \\ \eta &\equiv \frac{a^2\Lambda z_-}{1 + \frac{a^2\Lambda}{3}z_-}.\end{aligned}\tag{90}$$

In our calculations we used the following property for the values of Lauricella's multivariate function  $F_D$ :

$$\begin{aligned}F_D^{(n)}(\alpha, \beta_1, \dots, \beta_n, \gamma, 1, x_2, \dots, x_n) \\ = \frac{\Gamma(\gamma)\Gamma(\gamma - \alpha - \beta_1)}{\Gamma(\gamma - \alpha)\Gamma(\gamma - \beta_1)} F_D^{(n-1)}(\alpha, \beta_2, \dots, \beta_n, \gamma - \beta_1, x_2, \dots, x_n), \\ \max\{|x_2|, \dots, |x_n|\} < 1, \quad \Re(\gamma - \alpha - \beta_1) > 0.\end{aligned}\tag{91}$$

#### 5.4 Frame-dragging effect for polar non-spherical bound orbits in Kerr-Newman spacetime

Polar spherical orbits are characterised by the vanishing of the angular momentum of the particle, i.e.  $L = 0$ . We further assume in this section that  $\Lambda = 0$ . The relevant differential equation for the calculation of frame-dragging is:

$$\frac{d\phi}{dr} = \frac{(2ar - ae^2)E}{\Delta^{KN}\sqrt{R}}.\tag{92}$$

The quartic radial polynomial  $R$  is obtained from  $R'$  in (12) for  $\Lambda = L = 0$ . Using the partial fractions technique we integrate from the periastron distance  $r_P$  to the apoastron distance  $r_A$ :

Applying the transformation:

$$z = \frac{1}{\omega} \frac{r - \alpha_{\mu+1}}{r - \alpha_{\mu+2}} = \frac{\alpha - \gamma}{\alpha - \beta} \frac{r - \beta}{r - \gamma}\tag{93}$$

and organizing the roots of the radial polynomial and the radii of the event and Cauchy horizon in the ascending order of magnitude:

$$\alpha_\rho > \alpha_\sigma > \alpha_\nu > \alpha_i, \quad (94)$$

with the correspondence  $\alpha_\rho = \alpha_\mu = \alpha$ ,  $\alpha_\sigma = \alpha_{\mu+1} = \beta$ ,  $\alpha_\nu = \alpha_{\mu+2} = \gamma$ ,  $\alpha_i = \alpha_{\mu-i}$ ,  $i = 1, 2, 3$ ,  $\alpha_{\mu-1} = a_{\mu-2} = r_\pm$ ,  $\alpha_{\mu-3} = \delta$  we compute the exact analytic result in terms of Appell's hypergeometric function  $F_1$ :

$$\begin{aligned} \Delta\phi_{tpKN}^{GTR} = 2 & \left[ -\frac{\omega^{3/2}}{H_+} A_{tpKN}^+ F_1 \left( \frac{3}{2}, 1, \frac{1}{2}, 2, \kappa_+^{t2}, \kappa'^2 \right) \frac{\Gamma(\frac{3}{2}) \Gamma(\frac{1}{2})}{\Gamma(2)} \right. \\ & + \frac{\sqrt{\omega}}{H_+} A_{tpKN}^+ F_1 \left( \frac{1}{2}, 1, \frac{1}{2}, 1, \kappa_+^{t2}, \kappa'^2 \right) \frac{\Gamma^2(\frac{1}{2})}{\Gamma(1)} \\ & - \frac{\omega^{3/2}}{H_-} A_{tpKN}^- F_1 \left( \frac{3}{2}, 1, \frac{1}{2}, 2, \kappa_-^{t2}, \kappa'^2 \right) \frac{\Gamma(\frac{3}{2}) \Gamma(\frac{1}{2})}{\Gamma(2)} \\ & \left. + \frac{\sqrt{\omega}}{H_-} A_{tpKN}^- F_1 \left( \frac{1}{2}, 1, \frac{1}{2}, 1, \kappa_-^{t2}, \kappa'^2 \right) \frac{\Gamma^2(\frac{1}{2})}{\Gamma(1)} \right] \quad (95) \end{aligned}$$

where the partial fraction expansion parameters are given by:

$$A_{tpKN}^+ = \frac{-r_+ 2aE + ae^2 E}{r_- - r_+}, \quad A_{tpKN}^- = \frac{+r_- 2aE - ae^2 E}{r_- - r_+}. \quad (96)$$

The variables of the hypergeometric functions are given in terms of the roots of the quartic and the radii of the horizons by the expressions:

$$\kappa_\pm^{t2} := \frac{\alpha - \beta}{\alpha - \gamma} \frac{r_\pm - \gamma}{r_\pm - \beta}, \quad \kappa'^2 := \frac{\alpha - \beta}{\alpha - \gamma} \frac{\delta - \gamma}{\delta - \beta}, \quad (97)$$

while

$$\begin{aligned} H_\pm & \equiv \sqrt{(1-E^2)(\alpha_{\mu+1} - \alpha_{\mu-1})} \sqrt{\alpha_\mu - \alpha_{\mu+1}} \sqrt{\alpha_{\mu+1} - \alpha_{\mu-3}} \\ & = \sqrt{(1-E^2)(\beta - r_\pm)} \sqrt{\alpha - \beta} \sqrt{\beta - \delta}. \end{aligned} \quad (98)$$

#### 5.4.1 Exact calculation of the orbital period in non-spherical polar Kerr-Newman geodesics

In this section we will compute a novel exact formula for the orbital period for a test particle in a non-spherical polar Kerr-Newman geodesic. The relevant differential equation is:

$$\frac{cdt}{dr} = \frac{r^2 + a^2}{\Delta^{KN} \sqrt{R}} E(r^2 + a^2) - \frac{a^2 E \sin^2 \theta}{\sqrt{R}}, \quad (99)$$

and we integrate from periapsis to apoapsis and back to periapsis. Indeed, our analytic computation yields:

$$\begin{aligned}
ct \equiv cP_{KN} = & \frac{E\beta^2 2 \frac{GM}{c^2}}{\sqrt[2]{1-E^2} \sqrt[2]{\alpha-\gamma} \sqrt[2]{\beta-\delta}} \left[ \frac{\Gamma^2(1/2)}{\Gamma(1)} F_1 \left( \frac{1}{2}, 2, \frac{1}{2}, 1, \omega, \kappa^2 \right) \right. \\
& - \frac{2\omega\gamma}{\beta} \frac{\Gamma(3/2)\Gamma(1/2)}{\Gamma(2)} F_1 \left( \frac{3}{2}, 2, \frac{1}{2}, 2, \omega, \kappa^2 \right) + \frac{\gamma^2\omega^2}{\beta^2} \frac{\Gamma(5/2)\Gamma(1/2)}{\Gamma(3)} F_1 \left( \frac{5}{2}, 2, \frac{1}{2}, 3, \omega, \kappa^2 \right) \Big] \\
& + 2E(a^2 - e^2) \frac{GM}{c^2} \sqrt{\frac{\omega}{1-E^2}} \frac{1}{\sqrt[2]{(\alpha-\beta)(\beta-\delta)}} F(1/2, 1/2, 1, \kappa^2) \frac{\Gamma^2(1/2)}{\Gamma(1)} \\
& + \frac{4EGM}{c^2} \sqrt{\frac{\omega}{1-E^2}} \frac{\beta}{\sqrt[2]{(\alpha-\beta)(\beta-\delta)}} \left[ \frac{\Gamma^2(1/2)}{\Gamma(1)} F_1 \left( \frac{1}{2}, 1, \frac{1}{2}, 1, \omega, \kappa^2 \right) \right. \\
& - \frac{\omega\gamma}{\beta} F_1 \left( \frac{3}{2}, 1, \frac{1}{2}, 2, \omega, \kappa^2 \right) \frac{\Gamma(3/2)\Gamma(1/2)}{\Gamma(2)} \Big] \\
& + \frac{4EG2M}{c^2} \sqrt{\frac{\omega}{1-E^2}} \frac{1}{\sqrt[2]{(\alpha-\beta)(\beta-\delta)}} F(1/2, 1/2, 1, \kappa^2) \frac{\Gamma^2(1/2)}{\Gamma(1)} \\
& - \frac{4EG2M}{c^2} \left[ -\frac{\omega^{3/2} A_+^{KN}}{H_+} F_1 \left( \frac{3}{2}, 1, \frac{1}{2}, 2, \kappa_+^2, \mu^2 \right) \frac{\Gamma(3/2)\Gamma(1/2)}{\Gamma(2)} \right. \\
& + \frac{\omega^{1/2} A_+^{KN}}{H_+} F_1 \left( \frac{1}{2}, 1, \frac{1}{2}, 1, \kappa_+^2, \mu^2 \right) \frac{\Gamma^2(1/2)}{\Gamma(1)} - \frac{\omega^{3/2} A_-^{KN}}{H_-} F_1 \left( \frac{3}{2}, 1, \frac{1}{2}, 2, \kappa_-^2, \mu^2 \right) \frac{\Gamma(3/2)\Gamma(1/2)}{\Gamma(2)} \\
& + \left. \frac{\omega^{1/2} A_-^{KN}}{H_-} F_1 \left( \frac{1}{2}, 1, \frac{1}{2}, 1, \kappa_-^2, \mu^2 \right) \frac{\Gamma^2(1/2)}{\Gamma(1)} \right] \\
& + 2E \left[ -\frac{\omega^{3/2}(4e^2 r_+ - e^4)}{(-2\sqrt{1-a^2-e^2})H_+} F_1 \left( \frac{3}{2}, 1, \frac{1}{2}, 2, \kappa_+^2, \mu^2 \right) \frac{\Gamma(3/2)\Gamma(1/2)}{\Gamma(2)} \right. \\
& + \frac{\omega^{1/2}(4e^2 r_+ - e^4)}{(-2\sqrt{1-a^2-e^2})H_+} F_1 \left( \frac{1}{2}, 1, \frac{1}{2}, 1, \kappa_+^2, \mu^2 \right) \frac{\Gamma^2(1/2)}{\Gamma(1)} \\
& - \frac{\omega^{3/2}(e^4 - 4e^2 r_-)}{(-2\sqrt{1-a^2-e^2})H_-} F_1 \left( \frac{3}{2}, 1, \frac{1}{2}, 2, \kappa_-^2, \mu^2 \right) \frac{\Gamma(3/2)\Gamma(1/2)}{\Gamma(2)} \\
& + \left. \frac{\omega^{1/2}(e^4 - 4e^2 r_-)}{(-2\sqrt{1-a^2-e^2})H_-} F_1 \left( \frac{1}{2}, 1, \frac{1}{2}, 1, \kappa_-^2, \mu^2 \right) \frac{\Gamma^2(1/2)}{\Gamma(1)} \right] \\
& + \frac{-a^2 E \frac{GM}{c^2}}{\sqrt[2]{Q}} \left[ \sin(\varphi) F_1 \left( \frac{1}{2}, \frac{1}{2}, \frac{1}{2}, \frac{3}{2}, \sin^2 \varphi, \kappa^{2'} \sin^2 \varphi \right) + \left\{ -\sin(\varphi) F_1 \left( \frac{1}{2}, \frac{1}{2}, \frac{1}{2}, \frac{3}{2}, \sin^2 \varphi, \kappa^{2'} \sin^2 \varphi \right) \right. \right. \\
& + \left. \left. \sin(\varphi) F_1 \left( \frac{1}{2}, \frac{1}{2}, -\frac{1}{2}, \frac{3}{2}, \sin^2 \varphi, \kappa^{2'} \sin^2 \varphi \right) \right\} \times \frac{1}{\kappa^{2'}} \right] \quad (100)
\end{aligned}$$

where

$$\varphi = am \left( \sqrt[2]{Q} \frac{4}{\sqrt[2]{1-E^2}} \frac{1}{\sqrt[2]{\alpha-\gamma}} \frac{1}{\sqrt[2]{\beta-\delta}} \frac{\pi}{2} F \left( \frac{1}{2}, \frac{1}{2}, 1, \kappa^2 \right), \frac{a^2(1-E^2)}{Q} \right) \quad (101)$$

Parameters for the star <i>S2</i>	FD: $\Delta\phi_{tpKN}^{GTR}$	$P_{KN}(\text{yr})$	$LTP(\text{yr})$
$a = 0.52, e = 0.33, Q = 5693.30424, E = 0.999979485$	$\Delta\phi_{tpKN}^{GTR} = 3.14284 \frac{\text{arcsec}}{\text{revol.}}$	15.15	$6.25 \times 10^6$
$a = 0.52, e = 0.11, Q = 5693.30424, E = 0.999979485$	$\Delta\phi_{tpKN}^{GTR} = 3.14295 \frac{\text{arcsec}}{\text{revol.}}$	15.15	$6.25 \times 10^6$
$a = 0.52, e = 0, Q = 5693.30424, E = 0.999979485$	$\Delta\phi_{tpKN}^{GTR} = 3.14297 \frac{\text{arcsec}}{\text{revol.}}$	15.15	$6.25 \times 10^6$

Table 1: Lense-Thirring precession for the star *S2* in the central arcsecond of the galactic centre, using the exact formula (95). We assume a central galactic Kerr-Newman black hole with mass  $M_{\text{BH}} = 4.06 \times 10^6 M_{\odot}$  and that the orbit of *S2* star is a timelike non-spherical polar Kerr-Newman geodesic. The computation of the orbital period of the star *S2* was performed using the exact result in eqn.(100).

$$A_+^{KN} := -\frac{a^2 + e^2 - 2r'_+}{r'_- - r'_+}, \quad A_-^{KN} := -\frac{-a^2 - e^2 + 2r'_-}{r'_- - r'_+}, \quad (102)$$

and the moduli (variables) of the hypergeometric function of Appell are given by:

$$\begin{aligned} \mu^2 &= \kappa^2 = \frac{\alpha - \beta}{\alpha - \gamma} \frac{\delta - \gamma}{\delta - \beta} \\ \kappa_{\pm}^2 &= \frac{\alpha - \beta}{\alpha - \gamma} \frac{r'_{\pm} - \gamma}{r'_{\pm} - \beta}. \end{aligned} \quad (103)$$

For zero electric charge,  $e = 0$ , Eqn.(100) reduces correctly to Eqn.(33) in [6] for the case of a Kerr black hole. The Lense-Thirring period for a non-spherical polar timelike geodesic in Kerr-Newman BH geometry, is defined in terms of the Lense-Thirring precession Eq. (95) and its orbital period Eq. (100) as follows:

$$\text{LTP} := \frac{2\pi P_{KN}}{\Delta\phi_{tpKN}^{GTR}}. \quad (104)$$

We now proceed to calculate using our exact analytic solutions and assuming a central galactic Kerr-Newman black hole, the Lense-Thirring effect and the corresponding Lense-Thirring period for the observed stars *S2*, *S14* for various values of the Kerr parameter and the electric charge of the central black hole-see Tables 1-2. We observe that the contribution of the electric charge on the frame-dragging precession is small.

## 5.5 Periapsis advance for non-spherical polar timelike Kerr-Newman orbits

The purpose of this section is twofold. First, we apply closed form analytic expressions for the periapsis advance for non-constant radius orbits in Kerr-Newman spacetime, for the computation of this relativistic effect for the observed S-star orbits in the central arcsecond of SgrA\* supermassive black hole.



Parameters for the star <i>S14</i>	FD: $\Delta\phi_{tpKN}^{GTR}$	$P_{KN}(\text{yr})$	$LTP(\text{yr})$
$a = 0.9939, e = 0.11, Q = 5321.06355, E = 0.999988863$	$\Delta\phi_{tpKN}^{GTR} = 6.64977 \frac{\text{arcsec}}{\text{revol.}}$	37.88	$7.38 \times 10^6$
$a = 0.9939, e = 0, Q = 5321.06355, E = 0.999988863$	$\Delta\phi_{tpKN}^{GTR} = 6.64981 \frac{\text{arcsec}}{\text{revol.}}$	37.88	$7.38 \times 10^6$

Table 2: Lense-Thirring precession for the star *S14* in the central arcsecond of the galactic centre, using the exact formula (95). We assume a central galactic Kerr-Newman black hole with mass  $M_{\text{BH}} = 4.06 \times 10^6 M_{\odot}$  and that the orbit of *S14* star is a timelike non-spherical polar Kerr-Newman geodesic. The computation of the orbital period of the star *S14* was performed using the exact result in eqn.(100).

Secondly, this computation will provide us with realistic values for the first integrals of motion associated with non-circular orbits in KN and KN-(a)dS-spacetime. In principle, the latter values can be used as input in our analytic expressions for the redshift/blueshift experienced by photons emitted by test particles such as S-stars.

In [6] we computed a closed-form analytic expression for the periapsis advance that a non-spherical polar timelike orbit undergoes in Kerr spacetime in terms of Abel-Jacobi's amplitude function:

$$\begin{aligned} \Delta\Psi^{\text{GTR}} &= \Delta\Psi - 2\pi \\ &= \text{am} \left( \sqrt{Q} \frac{4}{\sqrt{1-E^2}} \frac{1}{\sqrt{\alpha-\gamma}} \frac{1}{\sqrt{\beta-\delta}} \frac{\pi}{2} F \left( \frac{1}{2}, \frac{1}{2}, 1, \kappa^2 \right), \frac{a^2(1-E^2)}{Q} \right) - 2\pi. \end{aligned} \quad (105)$$

The functional form of the solution will remain the same by incorporating the electric charge of the black hole, however the roots  $\alpha, \beta, \gamma, \delta$  will now be solutions of the quartic polynomial:

$$R = ((r^2 + a^2)E)^2 - (r^2 + a^2 + e^2 - 2r)(r^2 + Q + a^2E^2) = 0, \quad (106)$$

and thus they will differ from those of [6]. We compute with the aid of (105) the periapsis advance for the stars *S2* and *S14* assuming that they orbit in a timelike non-spherical polar Kerr-Newman geodesic. Our results are displayed in Tables 3 and 4. We observe that the effect of  $e$  is small.

We also computed with the aid of the exact formula Eqn. (103) in [8], the pericentre-shift for the stars *S2* and *S14* for various values for the spin and charge of the central black hole. By performing this calculation, we gain a more complete appreciation of the effect of the electric charge of the rotating galactic black hole (we assume that the KN solution describes the curved spacetime geometry around SgrA\*) on this observable. We also assume that the angular momentum axis of the orbit is co-aligned with the spin axis of the black hole and that the *S*-stars can be treated as neutral test particles i.e. their orbits are timelike non-circular equatorial Kerr-Newman geodesics. Our results are

Parameters for the star <i>S2</i>	Periastron advance $\Delta\Psi^{\text{GTR}}$
$a = 0.9939, e = 0.11, Q = 5693.30424, E = 0.999979485$	$\Delta\Psi_{\text{KN}}^{\text{GTR}} = 682.512 \frac{\text{arcsec}}{\text{revol.}}$
$a = 0.52, e = 0.11, Q = 5693.30424, E = 0.999979485$	$\Delta\Psi_{\text{KN}}^{\text{GTR}} = 682.533 \frac{\text{arcsec}}{\text{revol.}}$

Table 3: Periastron precession for the star *S2* in the central arcsecond of the galactic centre, using the exact formula (105) . We assume a central galactic Kerr-Newman black hole with mass  $M_{\text{BH}} = 4.06 \times 10^6 M_{\odot}$  and that the orbit of *S2* star is a timelike non-spherical polar Kerr-Newman geodesic.

Parameters for the star <i>S14</i>	Periastron advance $\Delta\Psi^{\text{GTR}}$
$a = 0.9939, e = 0.11, Q = 5321.06355, E = 0.999988863$	$\Delta\Psi_{\text{KN}}^{\text{GTR}} = 730.351 \frac{\text{arcsec}}{\text{revol.}}$
$a = 0.52, e = 0.11, Q = 5321.06355, E = 0.999988863$	$\Delta\Psi_{\text{KN}}^{\text{GTR}} = 730.376 \frac{\text{arcsec}}{\text{revol.}}$

Table 4: Periastron precession for the star *S14* in the central arcsecond of the galactic centre, using the exact formula (105) . We assume a central galactic Kerr-Newman black hole with mass  $M_{\text{BH}} = 4.06 \times 10^6 M_{\odot}$  and that the orbit of *S14* star is a timelike non-spherical polar Kerr-Newman geodesic.

displayed in Tables 5-8. It is evident in this case that the value of electric charge plays a significant role in the value of the pericentre-shift as opposed to the results in Tables 3 and 4<sup>9</sup>.

A few comments are in order. The values of the hypothetical electric charge of the central Kerr-Newman black hole have been chosen so that the surrounding spacetime represents a black hole, i.e. the singularity surrounded by the horizon, the electric charge and angular momentum  $J$  must be restricted by the relation:

$$\frac{GM}{c^2} \geq \left[ \left( \frac{J}{Mc} \right)^2 + \frac{Ge^2}{c^4} \right]^{1/2} \Leftrightarrow \quad (107)$$

$$\frac{GM}{c^2} \geq \left[ a^2 + \frac{Ge^2}{c^4} \right]^{1/2} \Rightarrow \quad (108)$$

$$e^2 \leq GM^2(1 - a'^2) \quad (109)$$

where in the last inequality  $a' = \frac{a}{GM/c^2}$  denotes a dimensionless Kerr parameter. Concerning the tentative values for the electric charge  $e$  we used in applying our exact solutions for the case of SgrA\* black hole we note that their likelihood is debatable: There is an expectation that the electric charge trapped in the galactic nucleus will not likely reach so high values as the ones close to the

<sup>9</sup>The parameters are consistent with data for the periastron, apoastron distances and orbital period for the stars *S2*, *S14* [4] (see also [6]).

Parameters for the star <i>S2</i>	Periastris advance $\delta_p^{teKN}$
$a = 0.9939, e = 0.11, L = 75.4539876, E = 0.999979485$	$\delta_p^{teKN} = 670.565 \frac{\text{arcsec}}{\text{revol.}}$
$a = 0.9939, e = 0.025, L = 75.4539876, E = 0.999979485$	$\delta_p^{teKN} = 671.876 \frac{\text{arcsec}}{\text{revol.}}$

Table 5: Periastron precession for the star *S2* in the central arcsecond of the galactic centre, using the exact formula Eqn. (103) in [8]. We assume a central galactic Kerr-Newman black hole with mass  $M_{\text{BH}} = 4.06 \times 10^6 M_\odot$  and that the orbit of the star *S2* is a timelike non-circular equatorial Kerr-Newman geodesic.

Parameters for the star <i>S14</i>	Periastris advance $\delta_p^{teKN}$
$a = 0.9939, e = 0.11, L = 72.9456205, E = 0.999988863$	$\delta_p^{teKN} = 717.128 \frac{\text{arcsec}}{\text{revol.}}$
$a = 0.9939, e = 0.025, L = 72.9456205, E = 0.999988863$	$\delta_p^{teKN} = 718.531 \frac{\text{arcsec}}{\text{revol.}}$

Table 6: Periastron precession for the star *S14* in the central arcsecond of the galactic centre, using the exact formula Eqn. (103) in [8]. We assume a central galactic Kerr-Newman black hole with mass  $M_{\text{BH}} = 4.06 \times 10^6 M_\odot$  and that the orbit of the star *S14* is a timelike non-circular equatorial Kerr-Newman geodesic.

extremal values predicted in (109) that allow the avoidance of a naked singularity. However, more precise statements on the electric charge's magnitude of the galactic black hole or its upper bound will only be reached once the relativistic effects predicted in this work are measured and a comparison of the theory we developed with experimental data will take place.

Parameters for the star <i>S2</i>	Periastris advance
$a = 0.52, e = 0.025, L = 75.4539876, E = 0.999979485$	$\delta_p^{teKN} = 677.571 \frac{\text{arcsec}}{\text{revol.}}$
$a = 0.52, e = 0.1, L = 75.4539876, E = 0.999979485$	$\delta_p^{teKN} = 676.5 \frac{\text{arcsec}}{\text{revol.}}$
$a = 0.52, e = 0.85, L = 75.4539876, E = 0.999979485$	$\delta_p^{teKN} = 595.1 \frac{\text{arcsec}}{\text{revol.}}$

Table 7: Periastron precession for the star *S2* in the central arcsecond of the galactic centre, using the exact formula Eqn. (103) in [8], for three different values of the electric charge of the galactic black hole. The Kerr parameter is  $a_{\text{Gal}} = 0.52 \frac{GM_{\text{BH}}}{c^2}$ . We assume a central KN black hole mass  $M_{\text{BH}} = 4.06 \times 10^6 M_\odot$  and that the orbit of the star *S2* is a timelike non-circular equatorial Kerr-Newman geodesic.

Parameters for the star <i>S14</i>	Periastron advance
$a = 0.52, e = 0.11, L = 72.9456205, E = 0.999988863$	$\delta_P^{teKN} = 723.432 \frac{\text{arcsec}}{\text{revol.}}$
$a = 0.52, e = 0.33, L = 72.9456205, E = 0.999988863$	$\delta_P^{teKN} = 711.595 \frac{\text{arcsec}}{\text{revol.}}$
$a = 0.52, e = 0.85, L = 72.9456205, E = 0.999988863$	$\delta_P^{teKN} = 636.568 \frac{\text{arcsec}}{\text{revol.}}$

Table 8: Periastron precession for the star *S14* in the central arcsecond of the galactic centre, using the exact formula Eqn. (103) in [8], for three different values of the electric charge of the galactic black hole. The Kerr parameter is  $a_{Gal} = 0.52 \frac{GM_{BH}}{c^2}$ . We assume a central black hole mass  $M_{BH} = 4.06 \times 10^6 M_\odot$

## 5.6 Periastron advance for non-spherical polar timelike Kerr-Newman -de Sitter orbits

In this section we are going to derive a new closed form expression for the pericentre-shift of a test particle in a timelike non-spherical polar Kerr-Newman-de Sitter geodesic.

After one complete revolution the angular integration has to satisfy the equation:

$$\int \frac{d\theta}{\sqrt{\Theta'}} = 2 \int_{r_A}^{r_P} \frac{dr}{\sqrt{R'}} = 2 \frac{\sqrt{\omega}}{\sqrt{\frac{\Lambda}{3}H}} \left[ -F_D \left( \frac{1}{2}, \frac{1}{2}, \frac{1}{2}, \frac{1}{2}, 1, \kappa^2, \lambda^2, \mu^2 \right) \frac{\Gamma(1/2)^2}{\Gamma(1)} \right. \\ \left. + \omega F_D \left( \frac{3}{2}, \frac{1}{2}, \frac{1}{2}, \frac{1}{2}, 2, \kappa^2, \lambda^2, \mu^2 \right) \frac{\Gamma(\frac{3}{2})\Gamma(\frac{1}{2})}{\Gamma(2)} \right] \quad (110)$$

For computing the radial hyperelliptic integral in (110)<sup>10</sup> in closed analytic form in terms of Lauricella's multivariable hypergeometric function  $F_D$ , we apply the transformation [6]:

$$z' = \frac{\alpha_{\mu-1} - \alpha_{\mu+1}}{\alpha_{\mu} - \alpha_{\mu+1}} \frac{r - \alpha_{\mu}}{r - \alpha_{\mu-1}} \quad (111)$$

The roots of the sextic radial polynomial are organised as follows:

$$\alpha_\nu > \alpha_\mu > \alpha_\rho > \alpha_i, \quad (112)$$

where  $\alpha_\nu = \alpha_{\mu-1}, \alpha_\rho = \alpha_{\mu+1} = r_P, \alpha_\mu = r_A, \alpha_i = \alpha_{\mu+i+1}, i = \overline{1, 3}$ . Also we define:

$$H \equiv \sqrt{(\alpha_\mu - \alpha_{\mu+1})(\alpha_\mu - \alpha_{\mu+2})(\alpha_\mu - \alpha_{\mu+3})(\alpha_\mu - \alpha_{\mu+4})}, \quad (113)$$

$$\omega := \frac{\alpha_\mu - \alpha_{\mu+1}}{\alpha_{\mu-1} - \alpha_{\mu+1}}. \quad (114)$$

<sup>10</sup>The sextic polynomial  $R'$  is obtained by setting  $\mu = 1$  and  $L = 0$  in (12).

The integral on the left of Eqn.(110) is an elliptic integral of the form:

$$\int \frac{d\theta}{\sqrt{\Theta'}} = -\frac{1}{2} \int \frac{dz}{\sqrt{z} \sqrt{a^4 \frac{\Lambda}{3} (z - z_\Lambda)(z - z_+)(z - z_-)}}, \quad (115)$$

Inverting the elliptic integral for  $z$  we obtain:

$$z = \frac{-\beta_1}{\omega_1 \text{sn}^2 \left( 2 \frac{\sqrt{\omega}}{\sqrt{\frac{\Lambda}{3} H}} \left[ -F_D \left( \frac{1}{2}, \beta, 1, \mathbf{x} \right) \frac{\Gamma(1/2)^2}{\Gamma(1)} + \omega F_D \left( \frac{3}{2}, \beta, 2, \mathbf{x} \right) \frac{\Gamma(\frac{3}{2})\Gamma(\frac{1}{2})}{\Gamma(2)} \right] \frac{\sqrt{\omega_1} \sqrt{\delta_1 - \beta_1} \sqrt{\alpha_1 - \beta_1} 2a^2}{2\omega_1} \sqrt{\frac{\Lambda}{3}}, \varkappa^2 \right) - 1}. \quad (116)$$

Equivalently the change in latitude after a complete radial oscillation leads to the following exact novel expression for the periastron advance for a test particle in an non-spherical polar Kerr-Newman-de Sitter orbit:

$$\theta = \arccos \pm \sqrt{z} =$$

$$\cos^{-1} \left( \pm \sqrt{\frac{-\beta_1}{\omega_1 \text{sn}^2 \left( 2 \frac{\sqrt{\omega}}{\sqrt{\frac{\Lambda}{3} H}} \left[ -F_D \left( \frac{1}{2}, \beta, 1, \mathbf{x} \right) \pi + \omega F_D \left( \frac{3}{2}, \beta, 2, \mathbf{x} \right) \frac{\Gamma(\frac{3}{2})\Gamma(\frac{1}{2})}{\Gamma(2)} \right] \frac{\sqrt{\delta_1 - \beta_1} \sqrt{\alpha_1 - \beta_1} a^2}{\sqrt{\omega_1}} \sqrt{\frac{\Lambda}{3}}, \varkappa^2 \right) - 1}} \right), \quad (117)$$

where:

$$\beta \equiv \left( \frac{1}{2}, \frac{1}{2}, \frac{1}{2} \right), \quad \mathbf{x} \equiv (\kappa^2, \lambda^2, \mu^2). \quad (118)$$

Also the Jacobi modulus  $\varkappa$  of the Jacobi's sinus amplitudinous elliptic function in formula (117), for the periapsis advance that a non-spherical polar orbit undergoes in the Kerr-Newman-de Sitter spacetime, is given in terms of the roots of the angular elliptic integral by:

$$\varkappa^2 = \frac{\omega_1 \delta_1}{\delta_1 - \beta_1} = \frac{\alpha_1 - \beta_1}{\alpha_1} \frac{\delta_1}{\delta_1 - \beta_1}. \quad (119)$$

The roots  $z_\Lambda, z_+, z_-$  appearing in (115) are roots of the polynomial equation:

$$z^3 \left( \frac{a^4 \Lambda}{3} \right) - z^2 \frac{a^2 \Lambda}{3} [Q + (L - aE)^2 \Xi^2] + a^2 \Xi z^2 (1 - E^2 \Xi) - z \{ [Q + (L - aE)^2 \Xi^2] \Xi + a^2 + 2aE \Xi^2 (L - aE) \} + Q = 0, \quad (120)$$

after setting <sup>11</sup>  $L = 0$ . Also the variables of the hypergeometric function  $F_D$  are:

---

<sup>11</sup>We have the correspondence  $\alpha_1 = z_+, \beta_1 = z_-, \delta_1 = z_\Lambda$ .

$$\begin{aligned}
\kappa^2 &= \omega \frac{\alpha_{\mu-1} - \alpha_{\mu+2}}{\alpha_{\mu} - \alpha_{\mu+2}} = \frac{\alpha - \beta}{r_{\Lambda}^1 - \beta} \frac{r_{\Lambda}^1 - \gamma}{\alpha - \gamma} \\
\lambda^2 &= \omega \frac{\alpha_{\mu-1} - \alpha_{\mu+3}}{\alpha_{\mu} - \alpha_{\mu+3}} = \frac{\alpha - \beta}{r_{\Lambda}^1 - \beta} \frac{r_{\Lambda}^1 - \delta}{\alpha - \delta} \\
\mu^2 &= \omega \frac{\alpha_{\mu-1} - \alpha_{\mu+4}}{\alpha_{\mu} - \alpha_{\mu+4}} = \frac{\alpha - \beta}{r_{\Lambda}^1 - \beta} \frac{r_{\Lambda}^1 - r_{\Lambda}^2}{\alpha - r_{\Lambda}^2}
\end{aligned} \tag{121}$$

## 5.7 Computation of first integrals for spherical timelike geodesics in Kerr-Newman spacetime

The equations determining the timelike orbits of constant radius in KN space-time are:

$$R = r^4 + (2Mr - e^2)(\eta_Q + (\xi - a)^2) + r^2(a^2 - \xi^2 - \eta_Q) - a^2\eta_Q - r^2 \frac{\Delta^{KN}}{E^2} = 0, \tag{122}$$

$$\frac{\partial R}{\partial r} = 4r^3 + 2M(\eta_Q + (\xi - a)^2) + 2r(a^2 - \xi^2 - \eta_Q) - 2r \frac{\Delta^{KN}}{E^2} - \frac{r^2}{E^2}(2r - 2M) = 0, \tag{123}$$

where we define:

$$\xi \equiv L/E, \quad \eta_Q \equiv \frac{Q}{E^2}. \tag{124}$$

Equations (122)-(123) can be combined to give:

$$\begin{aligned}
&3r^4 + a^2(r^2 - \frac{re^2}{M}) - \eta_Q(r^2 - a^2 - \frac{re^2}{M}) - \frac{r^2}{E^2}(3r^2 - 4rM + a^2 + e^2) \\
&+ \frac{re^2}{ME^2}(2r^2 - 3Mr + a^2 + e^2) - \frac{2e^2r^3}{M} = (r^2 - \frac{e^2r}{M})\xi^2,
\end{aligned} \tag{125}$$

$$\begin{aligned}
&r^4 + \eta_Q(a^2 - Mr + \frac{e^2r}{M}) - \frac{r^2}{E^2}r(r - M) - Mra^2 \\
&+ \frac{re^2}{ME^2}(2r - 3Mr + a^2 + e^2) - \frac{2e^2r^3}{M} = Mr(\xi^2 - 2a\xi) - \frac{e^2r}{M}\xi^2.
\end{aligned} \tag{126}$$

These equations can be solved for  $\xi$  and  $\eta_Q$ . Thus, eliminating  $\eta_Q$  between them, we obtain:

$$\begin{aligned}
&a^2(r - M)\xi^2 - 2aM(r^2 - a^2 - \frac{e^2r}{M})\xi \\
&- \left\{ (r^2 + a^2)[r(r^2 + a^2) - M(3r^2 - a^2)] + 2e^2r - \frac{a^2e^2}{M} \right\} + \frac{2a^2e^2r}{M}(r - \frac{e^2}{M}) + \frac{a^2e^4}{M^2} - \frac{(\Delta^{KN})^2}{E^2} \Big\} = 0.
\end{aligned} \tag{127}$$

We find that the solution of this quadratic equation is given by:

$$\xi = \frac{M(r^2 - a^2 - \frac{e^2 r}{M}) \pm r \Delta^{KN} \sqrt{1 - (1 - \frac{M}{r}) \frac{1}{E^2} - \frac{(e^2 - 2rM)e^2(r-M)a^2}{rM^2(\Delta^{KN})^2} - \frac{(r-M)(r^2 + a^2)a^2 e^2}{M(\Delta^{KN})^2 r^2}}}{a(r-M)}. \quad (128)$$

The parameter  $\eta_Q$  is then determined from equation:

$$\begin{aligned} -\eta_Q \left( r^2 - a^2 - \frac{re^2}{M} \right) &= -3r^4 - a^2 \left( r^2 - \frac{re^2}{M} \right) + \frac{r^2}{E^2} (3r^2 - 4rM + a^2 + e^2) \\ &- \frac{re^2}{ME^2} (2r^2 - 3Mr + a^2 + e^2) + \frac{2e^2 r^3}{M} + \left( r^2 - \frac{e^2 r}{M} \right) \xi^2. \end{aligned} \quad (129)$$

For zero electric charge  $e = 0$ , Equations (128) and (129) reduce correctly to the corresponding equations for the first integrals of motion in Kerr spacetime [43]:

$$\xi = \frac{M(r^2 - a^2) \pm r \Delta \sqrt{(1 - \frac{1}{E^2}(1 - \frac{M}{r}))}}{a(r-M)}, \quad (130)$$

$$\begin{aligned} \eta_Q a^2 (r-M) &= \frac{r^3}{M} [4a^2 M - r(r-3M)^2] - \frac{2r^3 M}{r-M} \Delta [1 \pm \sqrt{1 - \frac{1}{E^2}(1 - \frac{M}{r})}] \\ &+ \frac{r^2}{E^2} [r(r-2M)^2 - a^2 M]. \end{aligned} \quad (131)$$

## 5.8 The apparent impact factor for more general orbits

The apparent impact parameter  $\Phi$  for the Kerr-Newman-(anti) de Sitter black hole can also be computed in the case in which the considered orbits depart from the equatorial plane and therefore  $\theta \neq \pi/2$ . Again, we compute this quantity from the  $k^\mu k_\mu = 0$  relation just taking into account its maximum character, i.e., that  $k^r = 0$ . Our calculation yields:

$$\Phi_\gamma = \frac{-[a\Xi^2(r^2 + a^2) - a\Xi^2\Delta_r^{KN}] \pm \sqrt{\Xi^2\Delta_r^{KN}[\Xi^2 r^4 + \mathcal{Q}_\gamma(a^2 - \Delta_r^{KN})]}}{-a^2\Xi^2 + \Xi^2\Delta_r^{KN}}. \quad (132)$$

Our exact expression (132) for the apparent impact parameter in the KN(a)dS spacetime, for zero cosmological constant ( $\Lambda = 0$ ) and zero electric charge ( $e = 0$ ), reduces to eqn.(59) (the apparent impact parameter for the Kerr black hole) in [31]. Also for zero value for Carter's constant  $\mathcal{Q}_\gamma$  equation (132) reduces to eqn.(53).

## 6 Conclusions

In this work using the Killing-vector formalism and the associated first integrals we computed the redshift and blueshift of photons that are emitted by geodesic

massive particles and travel along null geodesics towards a distant observer-located at a finite distance from the KN(a)dS black hole. As a concrete example we calculated analytically the redshift and blueshift experienced by photons emitted by massive objects orbiting the Kerr-Newman-(anti) de Sitter black hole in equatorial and circular orbits, and following null geodesics towards a distant observer.

In addition and extending previous results in the literature we calculated in closed analytic form firstly, the frame-dragging that experience test particles in non-equatorial spherical timelike orbits in KN and KNdS spacetimes in terms of generalised hypergeometric functions of Appell and Lauricella. We also derived new exact results for the frame-dragging, pericentre-shift and orbital period for timelike non-spherical polar geodesics in Kerr-Newman spacetime and applied them for the computation of the corresponding relativistic effects for the orbits of stars S2 and S14 in the central arcsecond of SgrA\*, assuming the Galactic centre supermassive black hole is a Kerr-Newman black hole for various values of the Kerr parameter and electric charge. Secondly, we computed in closed analytic the periapsis advance for timelike non-spherical polar orbits in Kerr-Newman and Kerr-Newman de Sitter spacetimes. In the Kerr-Newman case, the pericentre-shift is expressed in terms of Jacobi's amplitude function and Gauß hypergeometric function, while in the Kerr-Newman-de Sitter the periapsis-shift is expressed in an elegant way in terms of Jacobi's sinus amplitudinis elliptic function  $\text{sn}$  and Lauricella's hypergeometric function  $F_D$  with three-variables.

We also computed the first integrals of motion for non-equatorial Kerr-Newman geodesics of constant radius. These expressions together with the analytic equation for the apparent impact factor we derived in this work-eqn (132), can be used to derive close form expressions for the redshift/blueshift of the emitted photons for such non-equatorial orbits in Kerr-Newman and Kerr-Newman (anti) de Sitter spacetimes. This will be a task for the future. Such a future endeavour will also involve the computation of the redshift/blueshift of the emitted photons for realistic values of the first integrals of motion associated with the observed orbits of S-stars (the emitters) such as those of Section 5.5, especially when the first measurements of the pericentre-shift of S2 will take place. The ultimate aim of course is to determine in a consistent way the parameters of the supermassive black hole that resides at the Galactic centre region SgrA\*.

It will also be interesting to investigate the effect of a massive scalar field on the orbit of S2 star and in particular on its redshift and periapsis advance by combining the results of this work and the exact solutions of the Klein-Gordon-Fock (KGF) equation on the KN(a)dS and KN black hole backgrounds in terms of Heun functions produced in [44] (see also [45]). This research will be the theme of a future publication <sup>12</sup>.

The fruitful synergy of theory and experiment in this fascinating research

---

<sup>12</sup>An initial study of such hypothetical scalar effects has been performed by Gravity Collaboration for the Kerr background and in solving approximately the KGF equation for the case in which the Compton wavelength of the scalar field is much larger than the gravitational radius of the black hole [46].



field will lead to the identification of the resident of the Milky Way's Galactic centre region and will provide an important test of General Relativity at the strong field regime.

**Acknowledgement 6** *I thank Dr. G. Kakarantzas for discussions.*

## A Linking the equatorial circular radii for emitter & detector

In this Appendix and for the case of a Kerr-Newman black hole we will show how the radii of the emitter and detector can be linked for circular equatorial orbits through the constants of motion  $L_\gamma, E_\gamma$ . The procedure was followed in [31] for the Kerr black hole. Indeed, from the fact that the first integrals of motion  $L_\gamma, E_\gamma$  and hence the apparent impact parameter  $\Phi$  are preserved along the whole trajectory followed by the photons, the latter quantity is the same when evaluated either at the emitter or detector positions, rendering the following relation  $\Phi_e = \Phi_d$ . For circular and equatorial orbits the maximised impact parameter for a Kerr-Newman black hole is given by the expression:

$$\Phi_\gamma = \frac{-a(2Mr - e^2) \pm r^2 \sqrt{r^2 + a^2 + e^2 - 2Mr}}{r^2 + e^2 - 2Mr}. \quad (133)$$

Its preservation provides the following equation that must be satisfied by the radius of a circular equatorial observer:

$$(r^2 - 2Mr + e^2) \times (r^4 + r^2(a^2 - \Phi_e) + 2Mr(\Phi_e - a)^2 - e^2(\Phi_e - a)^2) = 0 \quad (134)$$

The roots of the quartic equation in (134) can be obtained either by the Ferrari algorithm or in a more elegant way by the use of the Weierstraß functions making use of the addition theorem for points on the elliptic curve [8]:

$$\alpha = \frac{1}{2} \frac{\wp'(-x_1/2 + \omega) - \wp'(x_1)}{\wp(-x_1/2 + \omega) - \wp(x_1)}, \quad (135)$$

$$\beta = \frac{1}{2} \frac{\wp'(-x_1/2 + \omega + \omega') - \wp'(x_1)}{\wp(-x_1/2 + \omega + \omega') - \wp(x_1)}, \quad (136)$$

$$\gamma = \frac{1}{2} \frac{\wp'(-x_1/2 + \omega') - \wp'(x_1)}{\wp(-x_1/2 + \omega') - \wp(x_1)}, \quad (137)$$

$$\delta = \frac{1}{2} \frac{\wp'(-x_1/2) - \wp'(x_1)}{\wp(-x_1/2) - \wp(x_1)}, \quad (138)$$

where the point  $x_1$  is defined by the equation:

$$a^2 - \Phi^2 = -6\wp(x_1), \quad (139)$$

and  $\omega, \omega'$  denotes the half-periods of the elliptic function  $\wp$ . The equations

$$2(a - \Phi)^2 = 4\wp'(x_1), -3\wp^2(x_1) + g_2 = -e^2(\Phi - a)^2 \quad (140)$$

determine the Weierstraß invariants  $(g_2, g_3)$  with the result:

$$g_2 = \frac{1}{12}(a^2 - \Phi^2)^2 - e^2(\Phi - a)^2, \quad (141)$$

$$g_3 = -\frac{1}{216}(a^2 - \Phi^2)^3 - \frac{1}{4}(a - \Phi)^4 - e^2(\Phi - a)^2 \left( \frac{a^2 - \Phi^2}{6} \right). \quad (142)$$

The maximum root provides the circular radius of the detector. For zero electric charge,  $e = 0$  (i.e. Kerr black hole) the detector radius reduces to the result obtained in [31]:

$$\begin{aligned} r_d = \sqrt{\frac{\Phi_e - a}{3}} & \left[ \left( -\sqrt{27M^2(\Phi_e - a)} \right. \right. \\ & \left. \left. + \sqrt{27M^2(\Phi_e - a) + (\Phi_e + a)^3} \right)^{\frac{1}{3}} \right. \\ & \left. + (\Phi_e + a) \left( -\sqrt{27M^2(\Phi_e - a)} \right. \right. \\ & \left. \left. + \sqrt{27M^2(\Phi_e - a) + (\Phi_e + a)^3} \right)^{-\frac{1}{3}} \right]. \end{aligned} \quad (143)$$

## References

- [1] A. Einstein, Erklärung der Perihelbewegung des Merkur aus der allgemeinen Relativitätstheorie, Sitzungsberichte der Preussischen Akademie der Wissenschaften, (1915) 831.
- [2] A. M. Ghez *et al*, *Measuring distance and properties of the Milky Way's central supermassive black hole with stellar orbits*, Astrophys. J. **689**, (2008)1044, (arXiv:0808.2870), L. Meyer *et al*, *The Shortest-Known-Period Star Orbiting Our Galaxy's Supermassive Black Hole*, Science **338** (2012)84
- [3] R. Genzel *et al* 2010, *Rev.Mod. Phys.* **82** 3121-95, R. Schödel *et al*, *The nuclear cluster of Milky Way: our primary testbed for the interaction of a dense star cluster with a massive black hole* Class. Quantum Grav. **31** (2014) 244007
- [4] F. Eisenhauer *et al*, *Sinfoni in the galactic centre: young stars and infrared flares in the central light-month* (2005) Astrophys.J. **628** 246-59

- [5] C.M. Will, *Theory and Experiment in Gravitational Physics*, Cambridge University Press, Second Edition (2018)
- [6] G. V. Kraniotis, *Periapsis and gravitomagnetic precessions of stellar orbits in Kerr and Kerr-de Sitter black hole spacetimes*, Class. Quantum Grav. **24** (2007) 1775-1808;
- [7] G. V. Kraniotis *Precise analytic treatment of Kerr and Kerr-(anti) de Sitter black holes as gravitational lenses*, Class. Quant.Grav. **28** (2011) 085021
- [8] G. V. Kraniotis, *Gravitational lensing and frame dragging of light in the Kerr-Newman and the Kerr-Newman-(anti) de Sitter black hole spacetimes*, Gen. Rel. Grav. **46** (2014) 1818 [arXiv:1401.7118]
- [9] G. V. Kraniotis, *Frame-dragging and bending of light in Kerr and Kerr-(anti) de Sitter spacetimes*, Class.Quant.Grav. **22** (2005) 4391-4424
- [10] S. Zucker *et al*, *Probing post-Newtonian physics near the galactic black hole with stellar redshift measurements*, The Astrophysical Journal, 639: L21-L24 (2006)
- [11] Gravity Collaboration, *et al*, *Detection of the gravitational redshift in the orbit of the star S2 near the Galactic centre massive black hole* A&A 615,L15(2018)
- [12] T. Do *et al*, *Relativistic redshift of the star S0-2 orbiting the Galactic centre supermassive black hole*, arXiv:1907.10731[astro-ph.GA]
- [13] I. Waisberg *et al*, *What stellar orbit is needed to measure the spin of the Galactic centre black hole from astrometric data?*, Mon.Not.Roy.Astron.Soc. 476 (2018) no.3, 3600-3610
- [14] E. T. Newman, E. Couch, K. Chinnapared, A. Exton, A. Prakash and R. Torrence, *Metric of a Rotating, Charged Mass*, Journal of Mathematical Physics **6**, 918 (1965)
- [15] H. Ohanian and R. Ruffini 1994, *Gravitation and Spacetime* (New York: Norton and Company)
- [16] R P Kerr, *Gravitational field of a spinning mass as an example of algebraically special metrics*, Phys. Re. Lett. **11** (1963) 237
- [17] S. Perlmutter *et al*, Astrophys.Journal **517**(1999) 565; A. V. Filippenko *et al* Astron.J.**116** 1009
- [18] G. V. Kraniotis and S. B. Whitehouse, *General relativity, the cosmological constant and modular forms* Class. Quantum Grav. **19** (2002), 5073-5100
- [19] G. V. Kraniotis and S. B. Whitehouse, *Compact calculation of the perihelion precession of Mercury in general relativity the cosmological constant and Jacobi's inversion problem* Class. Quantum Grav. **20** (2003) 4817-4835

- [20] G. V. Kraniotis, *Precise relativistic orbits in Kerr and Kerr-(anti) de Sitter spacetimes*, Class.Quantum Grav. **21** (2004) 4743-4769
- [21] E. Hackmann, C. Lämmerzahl, *Geodesic equation in Schwarzschild-(anti-)de Sitter space-times: Analytical solutions and applications* Phys.Rev.D**78** (2008) 024035
- [22] Z.Stuchlík and J. Schee, *Comparison of general relativistic and pseudo-Newtonian description of Magellanic clouds motion in the field of Milky Way*, Int. J. of Mod.Phys.D **21** (2012)1250031; *Influence of the cosmological constant on the motion of Magellanic Clouds in the gravitational field of Milky Way* JCAP **9** (2011)018
- [23] J. Sultana, *Contribution of the cosmological constant to the bending of light in Kerr-de Sitter spacetime* Phys.Rev. D **88**, 042003 (2013)
- [24] The Event Horizon Telescope Collaboration, *First M87 Event Horizon Telescope Results. I. The Shadow of the Supermassive Black Hole*, The Astrophysical Journal Letters, 875: L1 (2019) April 10
- [25] E. Slaný, M. Pokorná and Z.Stuchlík, *Equatorial circular orbits in Kerr-anti-de Sitter spacetimes*, Gen. Rel.Grav. 45 (2013) 2611-2633
- [26] J.M. Bardeen, W.H. Press and S. P. Teukolsky, The Astrophys.Journal, **178**, (1972), 347-369
- [27] S. Soroushfar *et al*, Phys.Rev. D94 (2016) no.2, 024052
- [28] Z. Xu *et al*, *Kerr-Newman-AdS Black Hole In Quintessential Dark Energy*, Phys.Rev. D95 (2017) no.6, 064015
- [29] Z. Stuchlík and P. Slaný, *Equatorial circular orbits in the Kerr-de Sitter spacetimes*, Phys.Rev.D.**69**,064001 (2004)
- [30] G. V. Kraniotis, *Periapsis and gravitomagnetic precessions of stellar orbits in Kerr and Kerr-de Sitter black hole spacetimes*,Class. Quantum Grav. **24** (2007) 1775-1808; C. M. Will, ApJ, 674 (2008) L25, D. Merritt, T. Alexander, S. Mikkola and C. M. Will, Phys. Rev.D **81** (2010) 062002, L. Iorio,arXiv:1008.1720v4[gr-qc], also: Jaroszyński M. Acta Astronomica (1998) **48**, 653, G. F. Rubilar and A. Eckart (2001) A&A **374**, 95, P.C. Fragile and G. J. Mathews 2000, ApJ **542**, 328, N. N. Weinberg, M. Milosavljević and A. M. Ghez, (2005) ApJ **622**, 878, Preto M. and P. Saha (2009) ApJ **703**, 1743, G. V. Kraniotis, *Gravitational lensing and frame dragging of light in the Kerr-Newman and the Kerr-Newman-(anti) de Sitter black hole spacetimes*, Gen. Rel. Grav. **46** (2014) 1818 [arXiv:1401.7118], M. Grould *et al*, *General relativistic effects on the orbit of the S2 star with GRAVITY*A&A 608, A60 (2017), L. Iorio and F. Zhang, *On the post-Keplerian corrections to the orbital periods of a two-body system and their application to the Galactic Center*, Astrophys.J. 839

- (2017) no.1, 3, A. Hees *et al*, *Testing General Relativity with stellar orbits around the supermassive black hole in our Galactic center*, Phys.Rev.Lett. 118 (2017) no.21, 211101, Rong-Gen Cai, Tong-Bo Liu, , Shao-Jiang Wang, Commun.Theor.Phys. 70 (2018) no.6, 735-748, Gravity Collaboration, *Scalar field effects on the orbit of S2 star*, Mon.Not.Roy.Astron.Soc. 489 (2019) no.4, 4606-4621
- [31] A. Herrera-Aguilar, U. Nucamendi, *Kerr black hole parameters in terms of the redshift/blueshift of photons emitted by geodesic particles* Phys.Rev.D92 (2015) 045024
- [32] Preto M. and P. Saha (2009) ApJ **703**, 1743
- [33] G. Lauricella *Sulle funzioni ipergeometriche a più variabili*, Rend.Circ.Mat. Palermo **7** (1893) pp 111-158; P. Appell *Sur les fonctions hypergéométriques de deux variables*, J. Math.Pure Appl.**8** (1882) 173-216
- [34] M. Johnston and R. Ruffini, *Generalized Wilkins effect and selected orbits in a Kerr-Newman geometry*, Phys.Rev.D.**10** (1974) 2324-2329
- [35] B. P. Abbott *et al*, *Observation of Gravitational Waves from a Binary Black Hole Merger* Phys.Rev.Lett.**116**, 061102 (2016)
- [36] B. P. Abbott *et al*, *GW151226: Observation of Gravitational Waves from a 22-Solar-Mass Binary* Phys.Rev.Lett.**116**, 241103 (2016); B. P. Abbott *et al*, *GW170104: Observation of a 50-Solar-Mass Binary Black Hole Coalescence at Redshift 0.2* Phys. Rev. Lett.**118**, 221101 (2017); B. P. Abbott *et al*, *GW170814: A Three-Detector Observation of Gravitational Waves from a Binary Black Hole Coalescence* Phys.Rev.Lett.**119**, 141101 (2017); B. P. Abbott *et al*, *GW170817: Observation of Gravitational Waves from a Binary Neutron Star Inspiral* Phys.Rev.Lett.**119**, 161101 (2017)
- [37] Z. Stuchlík, G. Bao, E. Østgaard and S. Hledík, *Kerr-Newman-de Sitter black holes with a restricted repulsive barrier of equatorial photon motion*, Phys. Rev. D. **58** (1998) 084003
- [38] B. Carter, *Global structure of the Kerr family of gravitational fields* Phys.Rev.**174** (1968) 1559-71
- [39] Z. Stuchlík and S. Hledík, *Equatorial photon motion in the Kerr-Newman spacetimes with a non-zero cosmological constant*, Class. Quantum Grav. **17** (2000) 4541-4576
- [40] J. B. Griffiths and Jiří Podolský, *Exact spacetimes in Einstein's General Relativity*, Cambridge Monographs on Mathematical Physics, Cambridge University Press (2009)
- [41] Z. Stuchlík, *The motion of test particles in black-hole backgrounds with non-zero cosmological constant*, Bull. of the Astronomical Institute of Czechoslovakia **34** (1983) 129-149

- [42] M. Walker and R. Penrose, *On Quadratic First Integrals of the Geodesic Equations for Type 22 Spacetimes* , Commun. math. Phys. **18**, 265–274 (1970)
- [43] S. Chandrasekhar, *The Mathematical Theory of Black Holes* Oxford Classic Texts in Physical Sciences, 1992
- [44] G. V. Kraniotis, *The Klein-Gordon-Fock equation in the curved spacetime of the Kerr-Newman (anti) de Sitter black hole* Class. Quantum Grav. **33** (2016) 225011,[arXiv:1602.04830]; G. V. Kraniotis, CQG+ Insight: *The problem of perturbative charged massive scalar field in the Kerr-Newman-(anti) de Sitter black hole background*, 21/11/2016 and references therein
- [45] G. V. Kraniotis, *The massive Dirac equation in the Kerr-Newman-de Sitter and Kerr-Newman black hole spacetimes* J.Phys.Comm. **3** (2019) 035026,[arXiv:1801.03157 ]
- [46] Gravity Collaboration, *Scalar field effects on the orbit of S2 star*, Mon.Not.Roy.Astron.Soc. **489** (2019) no.4, 4606-4621